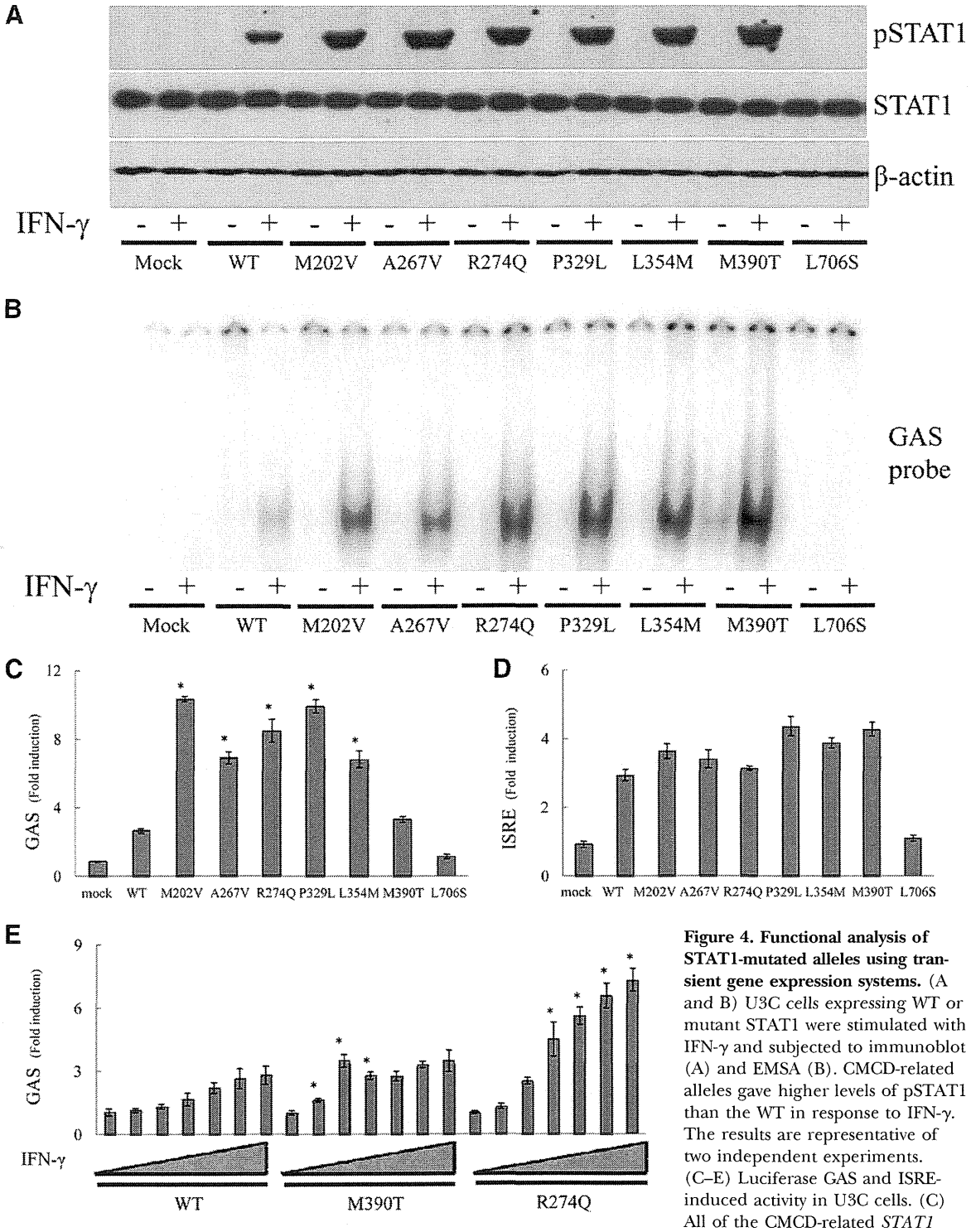

Figure 4. Functional analysis of STAT1-mutated alleles using transient gene expression systems. (A and B) U3C cells expressing WT or mutant STAT1 were stimulated with IFN-γ and subjected to immunoblot (A) and EMSA (B). CMCD-related alleles gave higher levels of pSTAT1 than the WT in response to IFN-γ. The results are representative of two independent experiments. (C–E) Luciferase GAS and ISRE-induced activity in U3C cells. (C) All of the CMCD-related *STAT1* mutations, except for M390T, were associated with levels of GAS transcriptional activity in response to IFN-γ, at least twice as high as those in cells transfected with the WT allele. (E) The M390T STAT1 behaved as a GOF protein in response to stimulation with low concentrations of IFN-γ. (D) An increase in ISRE induction in response to IFN-α was also observed in CMCD-related mutants, but this increase was much smaller than that observed for GAS induction. Differences were statistically significant in the cells expressing the mutants compared with the WT-expressing cells (*$P<0.05$).

overestimated here as a result of the limited number of cases in our cohort, but these results nevertheless strongly suggest that STAT1 GOF is the most frequent genetic etiology of CMCD among Japanese patients, accounting for at least one-half of these patients. The clinical penetrance of *STAT1* mutations appears to be extremely high, if not complete, as no individual with the morbid genotype but not CMCD has ever been identified [18–21, 35, 36]. We observed differences in clinical signs and severity, even between siblings with the same *STAT1* mutation. All of the mutated alleles, including three previously unknown mutations, were gain-of-phosphorylation and GOF in vitro in terms of GAS transcriptional activity. Moreover, all of these mutations affected residues in the CCD or DBD of STAT1. These results are highly consistent with previous findings [18–21, 35, 36].

Levels of pSTAT1 were found to be persistently high in the patients' $CD14^+$ monocytes by flow cytometric analysis. STAT1 does not appear to be hyperphosphorylated in lymphocytes but rather, in myeloid cells from patients with CMCD. A high level of pSTAT1 can be explained by the strong IFN-γR2 surface expression, specifically on monocytes, whereas IFN-γR1 is expressed ubiquitously [30]. The patients' cells had high basal levels of pSTAT1, a finding confirmed by immunoblot analysis of the patients' PBMCs. The amount of pSTAT1 in the cell is determined by the balance between pSTAT1 and STAT1 dephosphorylation [37]. CMCD-related mutations impair STAT1 nuclear dephosphorylation, potentially leading to some accumulation of pSTAT1 even in the absence of stimulation. Following stimulation with IFN-γ, $CD14^+$ monocytes contained significantly larger amounts of pSTAT1 than control cells. Moreover, this difference in pSTAT1 levels was even greater when staurosporine was added after IFN-γ stimulation. Higher levels of IFN-γ-induced pSTAT1 in monocytes of CMCD patients overlap with levels detected in cells from normal subjects, and the addition of staurosporine is required to discriminate the CMCD patients from control subjects. This technique is likely to be useful for the rapid assessment of STAT1 function in CMCD patients with unknown genetic etiology or those carrying functionally uncharacterized *STAT1* mutations. Furthermore, the results obtained are not affected by clinical diversity in the patients. Given the high frequency of GOF mutations of *STAT1*, the establishment of a rapid screening system based on STAT1 function should greatly facilitate the diagnosis of patients with CMCD.

Two patients presented atypical clinical signs in addition to CMCD. P1 suffered from cryptococcal meningitis, shingles, herpes simplex keratitis, and dermatitis. P6 presented severe, prolonged chicken-pox and chronic EBV infection. *Cryptococcus* is an opportunistic fungal pathogen, and IFN-γ signaling may play an important role in protective immunity against this microbe [38]. Indeed, IFN-γ administration increases the rate of clearance of HIV-associated cryptococcal infection from the cerebrospinal fluid when combined with antifungal drugs [39]. The CMCD-related *STAT1* mutations observed here were GOF in terms of IFN-γ-induced GAS transcriptional activity in vitro, so the cryptococcal meningitis observed in this patient is paradoxical. In addition to our study, recurrent cutaneous fusariosis and disseminated coccidioidomycosis and histoplasmosis have been reported in patients with GOF STAT1 mutation [40, 41]. Viral infections have also been reported in CMCD patients: one case of symptomatic cytomegalovirus infection and one familial case with recurrent herpes simplex virus and varicella infections have been reported [19, 25, 36]. STAT1 mediates the IFN-α/β-induced transcription of ISRE, which plays an important role in antiviral immunity. Therefore, severe viral infection is one of the typical symptoms in patients with AR STAT1 deficiency, which is caused by loss-of-function or hypomorphic mutations of *STAT1* [23, 32, 42–44]. As the CMCD-related *STAT1* mutations presented normal activity in terms of IFN-α-induced ISRE transcriptional activity in vitro, viral infections observed in two patients are also paradoxical. We observed higher levels of induction for *CXCL9* and *IRF1*, but not *ISG15*, in response to IFN-γ in $CD14^+$ monocytes from CMCD patients than in those from controls. These results suggest that *STAT1* GOF mutations may not induce an increase in the transcription of all downstream ISGs, potentially even causing paradoxical patterns of regulation for some target genes. There may be similar paradoxical responses to IFN-α/β, at least for some target genes. Moreover, a recent report suggests that the induction of CXCL9 and CXCL10 is impaired in STAT1-deficient U3A cells expressing GOF STAT1 alleles upon specific conditions, such as the restimulation with IFN-γ [41]. Further studies are required to determine whether and how *STAT1* GOF mutations confer a predisposition to pathogens, for which clearance generally requires normal IFN-γ and/or IFN-α signaling.

Surprisingly, a very recent report identified GOF mutations in *STAT1* in patients with *forkhead box P3* WT immune dysregulation, polyendocrinopathy, autoimmune enteropathy, and X-linked-like syndrome [25]. These patients present a broad, infectious phenotype that may be explained partially by progressive lymphopenia, finally resulting in hypogammaglobulinemia [26]. Although progressive lymphopenia was not observed, the patients in our cohort also presented a broad, infectious phenotype. Taken together with the clinical cases presented in our current study, these findings suggest that GOF mutations of *STAT1* may be associated with a much broader infectious phenotype than thought initially.

AUTHORSHIP

Y.M., M.T., S.O., O.H., and S.M. were involved in research design and data analysis. Y.M. and S.O. wrote the manuscript. K.I., N.H., H.M., S.K., Y.O., T. Imai, S.T., T.O., and T. Ito treated the patients. S.Y., Y.T., V.L.B., X-F.K., S.C., S.B-D., A.P., J-L.C., T.M., and M.K. directed experiments and edited the paper. S.O., T.M., and M.K. supervised all work.

ACKNOWLEDGMENTS

This study was supported, in part, by Grants-in-Aid for Scientific Research from the Japan Society for the Promotion of Science (22591161 to M.K.) and by Research on Measures for Intractable Diseases funding from the Japanese Ministry of

Health, Labor and Welfare (H22-Nanchi-ippan-078 to M.K.). This study was also supported, in part, by The Rockefeller University and grants from the National Center for Research Resources; National Center for Advancing Sciences (NCATS), U.S. National Institutes of Health (Grant Number 8UL1TR000043); and St. Giles Foundation. S.C. was supported by the AXA Research Fund and V.L.B and X-F.K., by the Stony Wold-Herbert Fund. Sequence analysis was supported by the Analysis Center of Life Science, Natural Science Center for Basic Research and Development, Hiroshima University. We thank Dr. Yoshiko Hasii (Osaka University) for referring patients. We thank Dusan Bogunovic, Alexandra Kreins, Marcela Moncada Velez, Ruben Martinez-Barricarte, and Michael Ciancanelli for helpful discussions and critical reading. We thank the members of the laboratory, Yelena Nemirovskaya and Eric Anderson, for secretarial assistance and Tiffany Nivare for technical assistance.

DISCLOSURES

The authors declare no conflict of interest.

REFERENCES

1. Kirkpatrick, C. H. (2001) Chronic mucocutaneous candidiasis. *Pediatr. Infect. Dis. J.* **20,** 197–206.
2. Lilic, D. (2002) New perspectives on the immunology of chronic mucocutaneous candidiasis. *Curr. Opin. Infect. Dis.* **15,** 143–147.
3. Minegishi, Y., Saito, M., Tsuchiya, S., Tsuge, I., Takada, H., Hara, T., Kawamura, N., Ariga, T., Pasic, S., Stojkovic, O., Metin, A., Karasuyama, H. (2007) Dominant-negative mutations in the DNA-binding domain of STAT3 cause hyper-IgE syndrome. *Nature* **448,** 1058–1062.
4. Holland, S. M., DeLeo, F. R., Elloumi, H. Z., Hsu, A. P., Uzel, G., Brodsky, N., Freeman, A. F., Demidowich, A., Davis, J., Turner, M. L., et al. (2007) STAT3 mutations in the hyper-IgE syndrome. *N. Engl. J. Med.* **357,** 1608–1619.
5. De Beaucoudrey, L., Samarina, A., Bustamante, J., Cobat, A., Boisson-Dupuis, S., Feinberg, J., Al-Muhsen, S., Jannière, L., Rose, Y., de Suremain, M., et al. (2010) Revisiting human IL-12Rβ1 deficiency: a survey of 141 patients from 30 countries. *Medicine (Baltimore)* **89,** 381–402.
6. Puel, A., Picard, C., Cypowyj, S., Lilic, D., Abel, L., Casanova, J. L. (2010) Inborn errors of mucocutaneous immunity to *Candida albicans* in humans: a role for IL-17 cytokines? *Curr. Opin. Immunol.* **22,** 467–474.
7. Minegishi, Y., Saito, M., Nagasawa, M., Takada, H., Hara, T., Tsuchiya, S., Agematsu, K., Yamada, M., Kawamura, N., Ariga, T., Tsuge, I., Karasuyama, H. (2009) Molecular explanation for the contradiction between systemic Th17 defect and localized bacterial infection in hyper-IgE syndrome. *J. Exp. Med.* **206,** 1291–1301.
8. De Beaucoudrey, L., Puel, A., Filipe-Santos, O., Cobat, A., Ghandil, P., Chrabieh, M., Feinberg, J., von Bernuth, H., Samarina, A., Janniere, L., et al. (2008) Mutations in STAT3 and IL12RB1 impair the development of human IL-17-producing T cells. *J. Exp. Med.* **205,** 1543–1550.
9. Milner, J. D., Brenchley, J. M., Laurence, A., Freeman, A. F., Hill, B. J., Elias, K. M., Kanno, Y., Spalding, C., Elloumi, H. Z., Paulson, M. L., Davis, J., Hsu, A., Asher, A. I., O'Shea, J., Holland, S. M., Paul, W. E., Douek, D. C. (2008) Impaired T(H)17 cell differentiation in subjects with autosomal dominant hyper-IgE syndrome. *Nature* **452,** 773–776.
10. Ma, C. S., Chew, G. Y., Simpson, N., Priyadarshi, A., Wong, M., Grimbacher, B., Fulcher, D. A., Tangye, S. G., Cook, M. C. (2008) Deficiency of Th17 cells in hyper IgE syndrome due to mutations in STAT3. *J. Exp. Med.* **205,** 1551–1557.
11. Kisand, K., Boe Wolff, A. S., Podkrajsek, K. T., Tserel, L., Link, M., Kisand, K. V., Ersvaer, E., Perheentupa, J., Erichsen, M. M., Bratanic, N., et al. (2010) Chronic mucocutaneous candidiasis in APECED or thymoma patients correlates with autoimmunity to Th17-associated cytokines. *J. Exp. Med.* **207,** 299–308.
12. Puel, A., Doffinger, R., Natividad, A., Chrabieh, M., Barcenas-Morales, G., Picard, C., Cobat, A., Ouachee-Chardin, M., Toulon, A., Bustamante, J., et al. (2010) Autoantibodies against IL-17A, IL-17F, and. IL-22 in patients with chronic mucocutaneous candidiasis and autoimmune polyendocrine syndrome type I. *J. Exp. Med.* **207,** 291–297.
13. Puel, A., Cypowyj, S., Bustamante, J., Wright, J. F., Liu, L., Lim, H. K., Migaud, M., Israel, L., Chrabieh, M., Audry, M., et al. (2011) Chronic mucocutaneous candidiasis in humans with inborn errors of interleukin-17 immunity. *Science* **332,** 65–68.
14. Cypowyj, S., Picard, C., Marodi, L., Casanova, J. L., Puel, A. (2012) Immunity to infection in IL-17-deficient mice and humans. *Eur. J. Immunol.* **42,** 2246–2254.
15. Marodi, L., Cypowyj, S., Toth, B., Chernyshova, L., Puel, A., Casanova, J. L. (2012) Molecular mechanisms of mucocutaneous immunity against *Candida* and *Staphylococcus* species. *J. Allergy Clin. Immunol.* **130,** 1019–1027.
16. Puel, A., Cypowyj, S., Marodi, L., Abel, L., Picard, C., Casanova, J. L. (2012) Inborn errors of human IL-17 immunity underlie chronic mucocutaneous candidiasis. *Curr. Opin. Allergy Clin. Immunol.* **12,** 616–622.
17. Alcais, A., Quintana-Murci, L., Thaler, D. S., Schurr, E., Abel, L., Casanova, J. L. (2010) Life-threatening infectious diseases of childhood: single-gene inborn errors of immunity? *Ann. N. Y. Acad. Sci.* **1214,** 18–33.
18. Liu, L., Okada, S., Kong, X. F., Kreins, A. Y., Cypowyj, S., Abhyankar, A., Toubiana, J., Itan, Y., Audry, M., Nitschke, P., et al. (2011) Gain-of-function human STAT1 mutations impair IL-17 immunity and underlie chronic mucocutaneous candidiasis. *J. Exp. Med.* **208,** 1635–1648.
19. Van de Veerdonk, F. L., Plantinga, T. S., Hoischen, A., Smeekens, S. P., Joosten, L. A., Gilissen, C., Arts, P., Rosentul, D. C., Carmichael, A. J., Smits-van der Graaf, C. A., Kullberg, B. J., van der Meer, J. W., Lilic, D., Veltman, J. A., Netea, M. G. (2011) STAT1 mutations in autosomal dominant chronic mucocutaneous candidiasis. *N. Engl. J. Med.* **365,** 54–61.
20. Takezaki, S., Yamada, M., Kato, M., Park, M. J., Maruyama, K., Yamazaki, Y., Chida, N., Ohara, O., Kobayashi, I., Ariga, T. (2012) Chronic mucocutaneous candidiasis caused by a gain-of-function mutation in the STAT1 DNA-binding domain. *J. Immunol.* **189,** 1521–1526.
21. Smeekens, S. P., Plantinga, T. S., van de Veerdonk, F. L., Heinhuis, B., Hoischen, A., Joosten, L. A., Arkwright, P. D., Gennery, A., Kullberg, B. J., Veltman, J. A., Lilic, D., van der Meer, J. W., Netea, M. G. (2011) STAT1 hyperphosphorylation and defective IL12R/IL23R signaling underlie defective immunity in autosomal dominant chronic mucocutaneous candidiasis. *PLoS One* **6,** e29248.
22. Chapgier, A., Boisson-Dupuis, S., Jouanguy, E., Vogt, G., Feinberg, J., Prochnicka-Chalufour, A., Casrouge, A., Yang, K., Soudais, C., Fieschi, C., et al. (2006) Novel STAT1 alleles in otherwise healthy patients with mycobacterial disease. *PLoS Genet.* **2,** e131.
23. Kong, X. F., Ciancanelli, M., Al-Hajjar, S., Alsina, L., Zumwalt, T., Bustamante, J., Feinberg, J., Audry, M., Prando, C., Bryant, V., et al. (2010) A novel form of human STAT1 deficiency impairing early but not late responses to interferons. *Blood* **116,** 5895–5906.
24. Tsumura, M., Okada, S., Sakai, H., Yasunaga, S., Ohtsubo, M., Murata, T., Obata, H., Yasumi, T., Kong, X. F., Abhyankar, A., et al. (2012) Dominant-negative STAT1 SH2 domain mutations in unrelated patients with Mendelian susceptibility to mycobacterial disease. *Hum. Mutat.* **33,** 1377–1387.
25. Uzel, G., Sampaio, E. P., Lawrence, M. G., Hsu, A. P., Hackett, M., Dorsey, M. J., Noel, R. J., Verbsky, J. W., Freeman, A. F., Janssen, E., et al. (2013) Dominant gain-of-function STAT1 mutations in FOXP3 wild-type immune dysregulation-polyendocrinopathy-enteropathy-X-linked-like syndrome. *J. Allergy Clin. Immunol.* **131,** 1611–1623.
26. Romberg, N., Morbach, H., Lawrence, M. G., Kim, S., Kang, I., Holland, S. M., Milner, J. D., Meffre, E. (2013) Gain-of-function STAT1 mutations are associated with PD-L1 overexpression and a defect in B-cell survival. *J. Allergy Clin. Immunol.* **131,** 1691–1693.
27. Bernabei, P., Coccia, E. M., Rigamonti, L., Bosticardo, M., Forni, G., Pestka, S., Krause, C. D., Battistini, A., Novelli, F. (2001) Interferon-γ receptor 2 expression as the deciding factor in human T, B, and myeloid cell proliferation or death. *J. Leukoc. Biol.* **70,** 950–960.
28. Bach, E. A., Aguet, M., Schreiber, R. D. (1997) The IFN γ receptor: a paradigm for cytokine receptor signaling. *Annu. Rev. Immunol.* **15,** 563–591.
29. Van Boxel-Dezaire, A. H., Stark, G. R. (2007) Cell type-specific signaling in response to interferon-γ. *Curr. Top. Microbiol. Immunol.* **316,** 119–154.
30. Kong, X. F., Vogt, G., Itan, Y., Macura-Biegun, A., Szaflarska, A., Kowalczyk, D., Chapgier, A., Abhyankar, A., Furthner, D., Khayat, C. D., et al. (2013) Haploinsufficiency at the human IFNGR2 locus contributes to mycobacterial disease. *Hum. Mol. Genet.* **22,** 769–781.
31. Fleisher, T. A., Dorman, S. E., Anderson, J. A., Vail, M., Brown, M. R., Holland, S. M. (1999) Detection of intracellular phosphorylated STAT-1 by flow cytometry. *Clin. Immunol.* **90,** 425–430.
32. Chapgier, A., Kong, X. F., Boisson-Dupuis, S., Jouanguy, E., Averbuch, D., Feinberg, J., Zhang, S. Y., Bustamante, J., Vogt, G., Le-

jeune, J., Mayola, E., de Beaucoudrey, L., Abel, L., Engelhard, D., Casanova, J. L. (2009) A partial form of recessive STAT1 deficiency in humans. *J. Clin. Invest.* **119,** 1502–1514.
33. Bogunovic, D., Byun, M., Durfee, L. A., Abhyankar, A., Sanal, O., Mansouri, D., Salem, S., Radovanovic, I., Grant, A. V., Adimi, P., et al. (2012) Mycobacterial disease and impaired IFN-γ immunity in humans with inherited ISG15 deficiency. *Science* **337,** 1684–1688.
34. Dupuis, S., Dargemont, C., Fieschi, C., Thomassin, N., Rosenzweig, S., Harris, J., Holland, S. M., Schreiber, R. D., Casanova, J. L. (2001) Impairment of mycobacterial but not viral immunity by a germline human STAT1 mutation. *Science* **293,** 300–303.
35. Hori, T., Ohnishi, H., Teramoto, T., Tsubouchi, K., Naiki, T., Hirose, Y., Ohara, O., Seishima, M., Kaneko, H., Fukao, T., Kondo, N. (2012) Autosomal-dominant chronic mucocutaneous candidiasis with STAT1-mutation can be complicated with chronic active hepatitis and hypothyroidism. *J. Clin. Immunol.* **32,** 1213–1220.
36. Toth, B., Mehes, L., Tasko, S., Szalai, Z., Tulassay, Z., Cypowyj, S., Casanova, J. L., Puel, A., Marodi, L. (2012) Herpes in STAT1 deficiency. *Lancet* **379,** 2500.
37. Ten Hoeve, J., de Jesus Ibarra-Sanchez, M., Fu, Y., Zhu, W., Tremblay, M., David, M., Shuai, K. (2002) Identification of a nuclear Stat1 protein tyrosine phosphatase. *Mol. Cell. Biol.* **22,** 5662–5668.
38. Chen, G. H., McDonald, R. A., Wells, J. C., Huffnagle, G. B., Lukacs, N. W., Toews, G. B. (2005) The γ interferon receptor is required for the protective pulmonary inflammatory response to *Cryptococcus neoformans*. *Infect. Immun.* **73,** 1788–1796.
39. Jarvis, J. N., Meintjes, G., Rebe, K., Williams, G. N., Bicanic, T., Williams, A., Schutz, C., Bekker, L. G., Wood, R., Harrison, T. S. (2012) Adjunctive interferon-γ immunotherapy for the treatment of HIV-associated cryptococcal meningitis: a randomized controlled trial. *AIDS* **26,** 1105–1113.
40. Wang, X., Lin, Z., Gao, L., Wang, A., Wan, Z., Chen, W., Yang, Y., Li, R. (2013) Exome sequencing reveals a signal transducer and activator of transcription 1 (STAT1) mutation in a child with recalcitrant cutaneous fusariosis. *J. Allergy Clin. Immunol.* **131,** 1242–1243.
41. Sampaio, E. P., Hsu, A. P., Pechacek, J., Bax, H. I., Dias, D. L., Paulson, M. L., Chandrasekaran, P., Rosen, L. B., Carvalho, D. S., Ding, L., et al. (2013) Signal transducer and activator of transcription 1 (STAT1) gain-of-function mutations and disseminated coccidioidomycosis and histoplasmosis. *J. Allergy Clin. Immunol.* **131,** 1624–1634.
42. Dupuis, S., Jouanguy, E., Al-Hajjar, S., Fieschi, C., Al-Mohsen, I. Z., Al-Jumaah, S., Yang, K., Chapgier, A., Eidenschenk, C., Eid, P., Al Ghonaium, A., Tufenkeji, H., Frayha, H., Al-Gazlan, S., Al-Rayes, H., Schreiber, R. D., Gresser, I., Casanova, J. L. (2003) Impaired response to interferon-α/β and lethal viral disease in human STAT1 deficiency. *Nat. Genet.* **33,** 388–391.
43. Chapgier, A., Wynn, R. F., Jouanguy, E., Filipe-Santos, O., Zhang, S., Feinberg, J., Hawkins, K., Casanova, J. L., Arkwright, P. D. (2006) Human complete Stat-1 deficiency is associated with defective type I and II IFN responses in vitro but immunity to some low virulence viruses in vivo. *J. Immunol.* **176,** 5078–5083.
44. Boisson-Dupuis, S., Kong, X. F., Okada, S., Cypowyj, S., Puel, A., Abel, L., Casanova, J. L. (2012) Inborn errors of human STAT1: allelic heterogeneity governs the diversity of immunological and infectious phenotypes. *Curr. Opin. Immunol.* **24,** 364–378.

KEY WORDS:
CMCD · STAT1 · GOF · pSTAT1

Genetic correction of *HAX1* in induced pluripotent stem cells from a patient with severe congenital neutropenia improves defective granulopoiesis

Tatsuya Morishima,[1] Ken-ichiro Watanabe,[1] Akira Niwa,[2] Hideyo Hirai,[3] Satoshi Saida,[1] Takayuki Tanaka,[2] Itaru Kato,[1] Katsutsugu Umeda,[1] Hidefumi Hiramatsu,[1] Megumu K. Saito,[2] Kousaku Matsubara,[4] Souichi Adachi,[5] Masao Kobayashi,[6] Tatsutoshi Nakahata,[2] and Toshio Heike[1]

[1]Department of Pediatrics, Graduate School of Medicine, Kyoto University, Kyoto; [2]Department of Clinical Application, Center for iPS Cell Research and Application, Kyoto University, Kyoto; [3]Department of Transfusion Medicine and Cell Therapy, Kyoto University Hospital, Kyoto; [4]Department of Pediatrics, Nishi-Kobe Medical Center, Kobe; [5]Human Health Sciences, Graduate School of Medicine, Kyoto University, Kyoto; and [6]Department of Pediatrics, Hiroshima University Graduate School of Biomedical Sciences, Hiroshima, Japan

ABSTRACT

HAX1 was identified as the gene responsible for the autosomal recessive type of severe congenital neutropenia. However, the connection between mutations in the *HAX1* gene and defective granulopoiesis in this disease has remained unclear, mainly due to the lack of a useful experimental model for this disease. In this study, we generated induced pluripotent stem cell lines from a patient presenting for severe congenital neutropenia with *HAX1* gene deficiency, and analyzed their *in vitro* neutrophil differentiation potential by using a novel serum- and feeder-free directed differentiation culture system. Cytostaining and flow cytometric analyses of myeloid cells differentiated from patient-derived induced pluripotent stem cells showed arrest at the myeloid progenitor stage and apoptotic predisposition, both of which replicated abnormal granulopoiesis. Moreover, lentiviral transduction of the *HAX1* cDNA into patient-derived induced pluripotent stem cells reversed disease-related abnormal granulopoiesis. This *in vitro* neutrophil differentiation system, which uses patient-derived induced pluripotent stem cells for disease investigation, may serve as a novel experimental model and a platform for high-throughput screening of drugs for various congenital neutrophil disorders in the future.

Introduction

Severe congenital neutropenia (SCN) is a rare myelopoietic disorder resulting in recurrent life-threatening infections due to a lack of mature neutrophils,[1] and individuals with SCN present for myeloid hypoplasia with an arrest of myelopoiesis at the promyelocyte/myelocyte stage.[1,2] SCN is actually a multigene syndrome that can be caused by inherited mutations in several genes. For instance, approximately 60% of SCN patients are known to carry autosomal dominant mutations in the *ELANE* gene, which encodes neutrophil elastase (NE).[3] An autosomal recessive type of SCN was first described by Kostmann in 1956,[4] and defined as Kostmann disease. Although the gene responsible for this classical type of SCN remained unknown for more than 50 years, Klein *et al.* identified mutations in *HAX1* to be responsible for this type of SCN in 2007.[5] HAX1 localizes predominantly to mitochondria, where it controls inner mitochondrial membrane potential ($\Delta\psi_m$) and apoptosis.[6,7] Although an increase in apoptosis in mature neutrophils was presumed to cause neutropenia in HAX1 gene deficiency,[5] the connection between *HAX1* gene mutations and defective granulopoiesis in SCN has remained unclear.

To control infections, SCN patients are generally treated with granulocyte colony-stimulating factor (G-CSF); however, long-term G-CSF therapy associates with an increased risk of myelodysplastic syndrome and acute myeloid leukemia (MDS/AML).[8,9] Although hematopoietic stem cell transplantations are available as the only curative therapy for this disease, they can result in various complications and mortality.[4]

Many murine models of human congenital and acquired diseases are invaluable for disease investigation as well as for novel drug discoveries. However, their use in a research setting can be limited if they fail to mimic strictly the phenotype of the human disease in question. For instance, the *Hax1* knock-out mouse is characterized by lymphocyte loss and neuronal apoptosis, but not neutropenia.[10] Thus, it is not a suitable experimental model for SCN. Induced pluripotent stem (iPS) cells are reprogrammed somatic cells with embryonic stem (ES) cell-like characteristics produced by the introduction of specific transcription factors,[11,16] and they may substitute murine models of human disease. It is believed that iPS cell technology, which generates disease-specific pluripotent stem cells in combination with directed cell differentiation, will contribute enormously to patient-oriented research, including disease pathophysiology, drug screening, cell transplantation, and gene therapy.

In vitro neutrophil differentiation systems, which can reproduce the differentiation of myeloid progenitor cells to mature neutrophils, are needed to understand the pathogenesis of SCN better. Recently, we established a neutrophil differentia-

 doi:10.3324/haematol.2013.083873
The online version of this article has a Supplementary Appendix.
Manuscript received on January 9, 2013. Manuscript accepted on August 20, 2013.
Correspondence: heike@kuhp.kyoto-u.ac.jp

tion system from human iPS cells[17] as well as a serum- and feeder-free monolayer hematopoietic culture system from human ES and iPS cells.[18] In this study, we generate iPS cell lines from an SCN patient with *HAX1* gene deficiency and differentiate them into neutrophils *in vitro*. Furthermore, we corrected for the *HAX1* gene deficiency in HAX1-iPS cells by lentiviral transduction with *HAX1* cDNA and analyzed the neutrophil differentiation potential of these cells. Thus, this *in vitro* neutrophil differentiation system from patient-derived iPS cells may be a useful model for future studies in SCN patients with *HAX1* gene deficiency.

Methods

Human iPS cell generation

Skin biopsy specimens were obtained from an 11-year old male SCN patient with *HAX1* gene deficiency.[19] This study was approved by the Ethics Committee of Kyoto University, and informed consent was obtained from the patient's guardians in accordance with the Declaration of Helsinki. Fibroblasts were expanded in DMEM (Nacalai Tesque, Inc., Kyoto, Japan) containing 10% FBS (vol/vol, Invitrogen, Carlsbad, CA, USA) and 0.5% penicillin and streptomycin (wt/vol, Invitrogen). Generation of iPS cells was performed as described previously.[12] In brief, we introduced *OCT3/4, SOX2, KLF4*, and *cMYC* using ecotropic retroviral transduction into patient's fibroblasts expressing mouse *Slc7a1*. Six days after transduction, cells were harvested and re-plated onto mitotically inactive SNL feeder cells. On the following day, DMEM was replaced with primate ES cell medium (ReproCELL, Kanagawa, Japan) supplemented with basic fibroblast growth factor (5 ng/mL, R&D Systems, Minneapolis, MN, USA). Three weeks later, individual colonies were isolated and expanded.

Maintenance of cells

Control ES (KhES-1) and control iPS (253G4 and 201B6) cells were kindly provided by Drs. Norio Nakatsuji and Shinya Yamanaka (Kyoto University, Kyoto, Japan), respectively. These human ES and iPS cell lines were maintained on mitomycin-C (Kyowa Hakko Kirin, Tokyo, Japan)-treated SNL feeder cells as described previously[17] and subcultured onto new SNL feeder cells every seven days.

Flow cytometric analysis

Cells were stained with antibodies as reported previously.[17] Samples were analyzed using an LSR flow cytometer and Cell Quest software (Becton-Dickinson).

Neutrophil differentiation of iPS cells

In a previous study, we established a serum and feeder-free monolayer hematopoietic culture system from human ES and iPS cells.[18] In this study, we modified this culture system to direct neutrophil differentiation. iPS cell colonies were cultured on growth factor-reduced Matrigel (Becton-Dickinson)-coated cell culture dishes in Stemline II hematopoietic stem cell expansion medium (Sigma-Aldrich, St. Louis, MO, USA) containing the insulin-transferrin-selenium (ITS) supplement (Invitrogen) and cytokines. iPS cells were treated with cytokines as follows: bone morphogenetic protein (BMP) 4 (20 ng/mL, R&D Systems) was added for four days and then replaced with vascular endothelial growth factor (VEGF) 165 (40 ng/mL, R&D Systems) on Day 4. On Day 6, VEGF 165 was replaced with a combination of stem cell factor (SCF, 50 ng/mL, R&D Systems), interleukin (IL)-3 (50 ng/mL, R&D Systems), thrombopoietin (TPO, 5 ng/mL, kindly provided by Kyowa Hakko Kirin), and G-CSF (50 ng/mL, also kindly provided by Kyowa Hakko Kirin). Thereafter, medium was replaced every five days.

Dead cell removal and CD45$^+$ leukocyte separation

Floating cells were collected, followed by the removal of dead cells and cellular debris with the Dead Cell Removal kit (Miltenyi Biotec, Bergisch Gladbach, Germany). CD45$^+$ cells were then separated using human CD45 microbeads (Miltenyi Biotec). Cell separation procedures were performed using the autoMACS Pro Separator (Miltenyi Biotec).

Statistical analysis

Statistical analysis was carried out using Student's t-test. $P<0.05$ was considered statistically significant.

Results

Generation of iPS cell lines from an SCN patient with HAX1 gene deficiency

To generate patient-derived iPS cell lines, dermal fibroblasts were obtained from a male SCN patient with a homozygous 256C-to-T transition resulting in an R86X mutation in the *HAX1* gene.[19] These fibroblasts were reprogrammed to iPS cells after transduction with retroviral vectors encoding *OCT3/4, SOX2, KLF4* and *cMYC*,[12] and a total of 11 iPS cell clones were obtained. From these, we randomly selected three clones for propagation and subsequent analyses. One of these clones (HAX1 4F5) was generated with four factors (*OCT3/4, SOX2, KLF4*, and *cMYC*); the remaining clones (HAX1 3F3 and 3F5) were generated with three factors (*OCT3/4, SOX2*, and *KLF4*).[12]

All of these patient-derived iPS cell clones showed a characteristic human ES cell-like morphology (Figure 1A), and they propagated for serial passages in human ES cell maintenance culture medium. Quantitative PCR analysis showed the expression of *NANOG*, a pluripotent marker gene, to be comparable to that of control ES (KhES-1) and iPS (253G4 and 201B6) cells (Figure 1B). Surface marker analysis indicated that they were also positive for SSEA4, a human ES and iPS cell marker (Figure 1C). DNA sequencing analysis verified an identical mutation in the *HAX1* gene in all established iPS cell clones (Figure 1D). The pluripotency of all iPS cell clones was confirmed by the presence of cell derivatives representing all three germ layers by teratoma formation after subcutaneous injection of undifferentiated iPS cells into immunocompromised NOD/SCID/γc^{null} mice (Figure 1E).

To validate the authenticity of iPS cells further, we investigated the expression of the four genes that were used for iPS cell generation. The expression level of all endogenous genes was comparable to control ES and iPS cells. On the other hand, transgene expression was largely undetectable in patient-derived iPS cell clones (*Online Supplementary Figure S1A*). Chromosomal analysis revealed that all patient-derived iPS cell clones maintained a normal karyotype (*Online Supplementary Figure S1B*). Genetic identity was shown by short tandem repeat analysis (*Online Supplementary Figure S1C*).

Taken collectively, these results indicate that iPS cell clones were comprised of good quality iPS cells derived from the somatic cells of an SCN patient with *HAX1* gene deficiency (HAX1-iPS cells).

Maturation arrest at the progenitor level in neutrophil differentiation from HAX1-iPS cells

The paucity of mature neutrophils in the peripheral blood and a maturation arrest at the promyelocyte/myelocyte stage in the bone marrow are characteristic laboratory findings presented in the SCN patients with *HAX1* gene deficiency. To investigate whether our patient-derived iPS cell model accurately replicated this disease phenotype, we assessed neutrophil differentiation from HAX1-iPS cells by using a serum- and feeder-free monolayer culture system[18] with minor modifications (Online *Supplementary Figure S2*).

In this system, we cultured iPS cell colonies on Matrigel-coated dishes in serum-free medium supplemented with several cytokines and obtained hematopoietic cells as floating cells on approximately Day 26 of differentiation. May-Giemsa staining of floating live $CD45^+$ cells derived from normal iPS cells showed that approximately 40% were mature neutrophils (Figure 2A and B). The remaining cells consisted of immature myeloid cells as well as a small number of macrophages. Cells of other lineages such as erythroid or lymphoid cells were not observed. On the other hand, HAX1-iPS cell-derived blood cells contained only approximately 10% mature neutrophils and approxi-

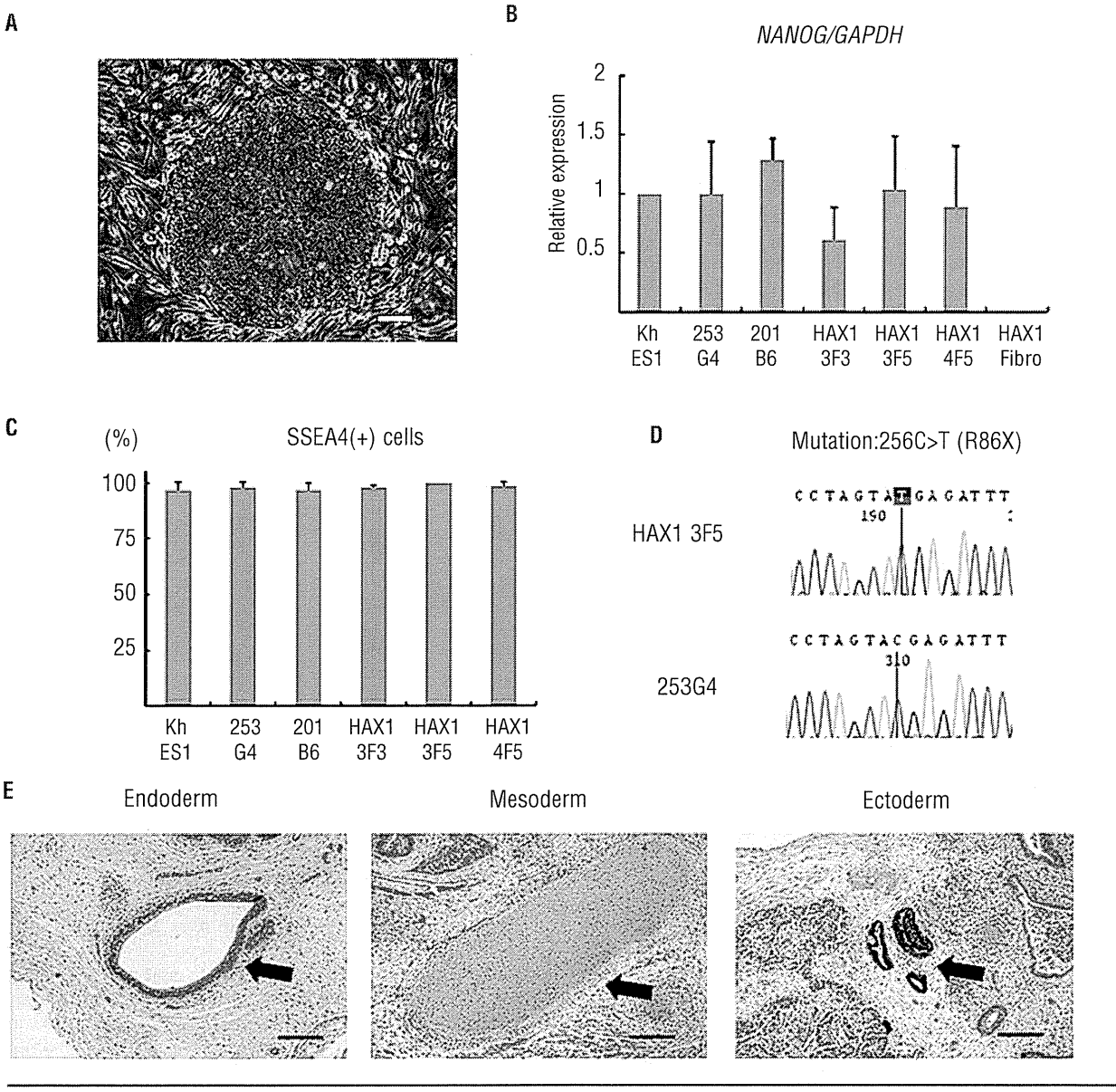

Figure 1. Generation of iPS cell lines from an SCN patient with *HAX1* gene deficiency. (A) Human ES cell-like morphology of HAX1-iPS cells. Scale bar: 200 μm. (B) *NANOG* expression in HAX1-iPS cells, control iPS cells (253G4 and 201B6), and patient-derived fibroblasts (HAX1 Fibro) compared to control ES cells (KhES1). *GAPDH* was used as an internal control (n = 3; bars represent SDs). (C) SSEA-4 expression analysis using flow cytometry. Gated on $TRA1\text{-}85^+DAPI^-$ cells as viable human iPS (ES) cells (n = 3; bars represent SDs). (D) DNA sequencing analysis of the *HAX1* gene in iPS cells. HAX1-iPS cells showed 256C>T (R86X) mutation that was found in the patient. (E) Teratoma formation from HAX1-iPS cells in the NOD/SCID/γc^{null} (NOG) mouse. Arrows indicate the following; Endoderm: respiratory epithelium; Mesoderm: cartilage; Ectoderm: pigmented epithelium. Scale bars: 200 μm. (A, D-E) Representative data (HAX1 3F5) are shown.

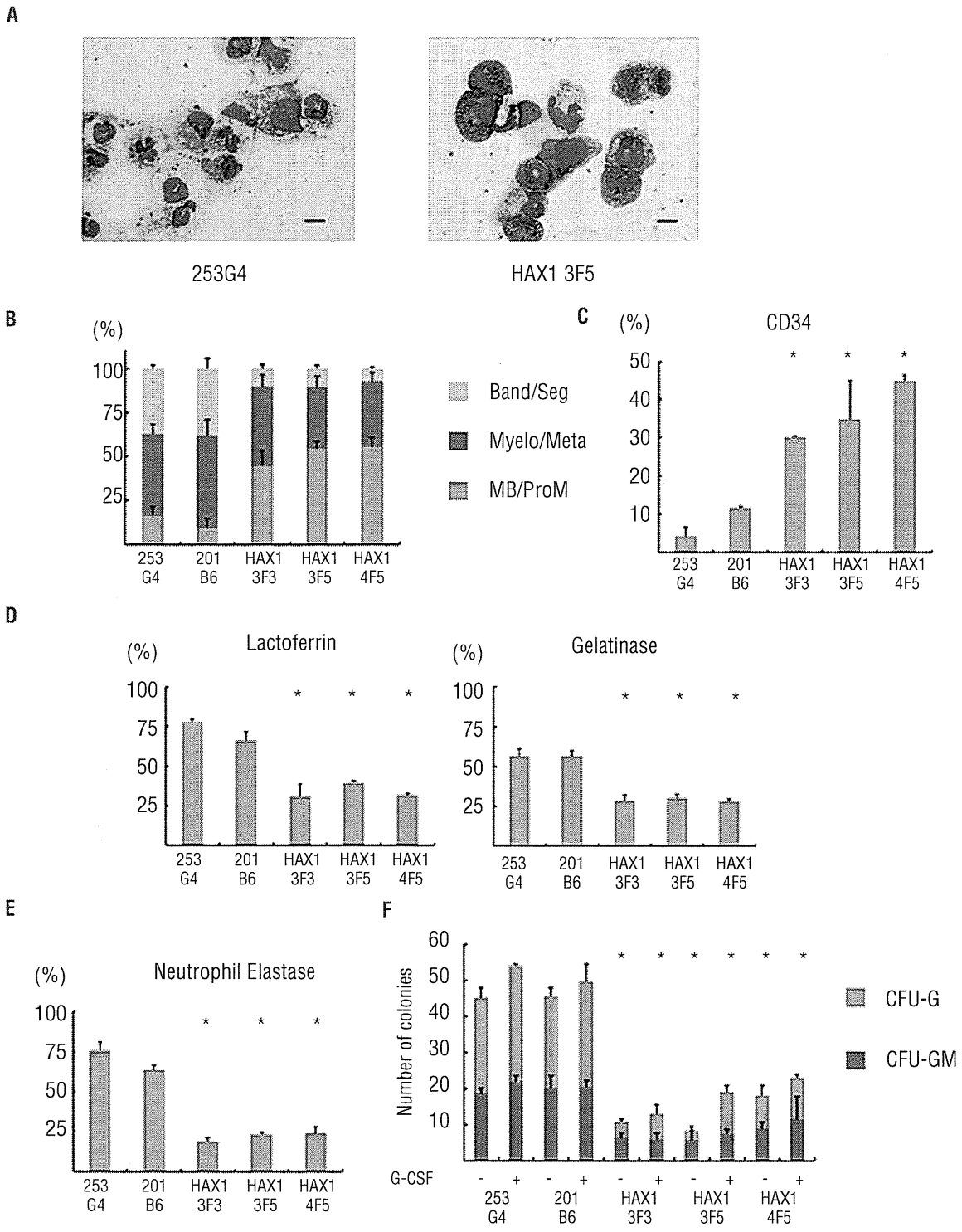

Figure 2. Maturation arrest at the progenitor level in neutrophil differentiation from HAX1-iPS cells. (A) May-Giemsa staining of CD45$^+$ cells derived from normal (253G4) and HAX1-iPS (HAX1 3F5) cells. Scale bars: 10 μm. (B) Morphological classification of CD45$^+$ cells derived from iPS cells. Cells were classified into three groups: myeloblast and promyelocyte (MB/ProM), myelocyte and metamyelocyte (Myelo/Meta), and band and segmented neutrophils (Band/Seg) (n = 3; bars represent SDs). (C) Flow cytometric analysis of CD45$^+$ cells derived from iPS cells. Cells gated on human CD45$^+$ DAPI$^-$ were analyzed (n = 3; bars represent SDs; *P<0.05 compared to control iPS cells). (D) Immunocytochemical analysis of CD45$^+$ cells derived from iPS cells (n = 3; bars represent SDs; *P<0.05 compared to control iPS cells). (E) NE staining of CD45$^+$ cells derived from iPS cells (n = 3; bars represent SDs; *P<0.05 compared to control iPS cells). (F) Colony-forming assay of cells derived from iPS cells. On Day 16, living adherent cells were collected and cultured in methylcellulose medium (see *Online Supplementary Appendix*). The number of colonies generated from 1×10^4 cells is indicated (n = 3; bars represent SD; *P<0.05 compared to control iPS cells). (A–E) Live CD45$^+$ cells derived from normal and HAX1-iPS cells on Day 26 of neutrophil differentiation were analyzed. Dead cells and CD45$^-$ cells were depleted using an autoMACS Pro separator (see *Methods*).

mately 50% immature myeloid cells, including myeloblasts and promyelocytes (Figure 2A and B). Flow cytometric analysis revealed that the percentage of $CD34^+$ cells within HAX1-iPS cell-derived blood cells was significantly higher than in normal iPS cell-derived blood cells (Figure 2C), which also showed that the percentage of phenotypically immature myeloid cells was higher in HAX1-iPS cell-derived blood cells than in normal iPS cell-derived blood cells.

Immunocytochemical analysis for lactoferrin and gelatinase, which are constitutive proteins of neutrophil specific granules observed in mature neutrophils, showed that the proportion of these granule-positive cells was significantly lower in HAX1-iPS cell-derived blood cells than in normal iPS cell-derived blood cells (Figure 2D). NE is a protease stored in primary granules of neutrophilic granulocytes that are formed at the promyelocytic phase of granulocyte differentiation. *ELANE* mRNA expression in myeloid progenitors and the protein level of NE in plasma are markedly reduced in SCN patients with mutations in *ELANE* or *HAX1*.[20] Consistent with this, the proportion of NE-positive cells was significantly lower in blood cells derived from HAX1-iPS cells than in those derived from normal iPS cells (Figure 2E). Thus, the level of functionally mature neutrophils decreased during *in vitro* granulopoietic differentiation of HAX1-iPS cells.

Next, we analyzed the colony-forming potential of HAX1-iPS cell-derived myeloprogenitor cells. Significantly fewer colonies, which were classified as granulocyte-macrophage (GM) or granulocyte (G) colony-forming units (CFU), were derived from HAX1-iPS cells than from control iPS cells. Furthermore, the colonies derived from HAX1-iPS cells were predominantly CFU-GM (Figure 2F). Thus, maturation arrest occurred at the clonogenic progenitor stage during *in vitro* neutrophil differentiation of HAX1-iPS cells.

SCN is characterized by severe neutropenia with very low absolute neutrophil counts in peripheral blood, and many SCN patients respond to G-CSF treatment.[1,2] In colony-forming assays using bone marrow cells of SCN patients, primitive myeloid progenitor cells have reduced responsiveness to hematopoietic cytokines including G-CSF.[21,22] Therefore, we next examined the response of HAX1-iPS cell-derived blood cells to G-CSF using a colony-forming assay. Although the number of colonies derived from HAX1-iPS cells slightly increased following the addition of G-CSF, it remained significantly lower than the number of colonies derived from control iPS cells in the absence of G-CSF (Figure 2F). These results indicate that the responsiveness of HAX1-iPS-derived blood cells to G-CSF was insufficient to restore the neutrophil count to a normal level and are consistent with the fact that the absolute neutrophil counts of SCN patients remain low following G-CSF therapy.[19,21]

Neutrophils derived from HAX1-iPS cells are predisposed to undergo apoptosis due to their reduced $\Delta\psi_m$

Previous studies have shown HAX1 to localize to mitochondria[6] and to mediate anti-apoptotic activity.[7] Interestingly, this apoptotic predisposition of neutrophils due to their reduced $\Delta\psi_m$ was observed in HAX1-deficient patients,[5] prompting us to examine apoptosis in HAX1-iPS cell-derived blood cells. Consistent with these reports, HAX1-iPS cell-derived blood cells showed a significantly higher percentage of Annexin V-positive cells than in control cells (Figure 3A). In addition, a mitochondrial membrane potential assay revealed that the percentage of cells with a low $\Delta\psi_m$ was significantly higher in HAX1-iPS cell-derived blood cells than in blood cells derived from control iPS cells (Figure 3B). By contrast, the percentage of cells with a low $\Delta\psi_m$ was similar in undifferentiated HAX1-iPS cells and undifferentiated control iPS cells (*Online Supplementary Figure S3*).

Thus, increased apoptosis due to reduced $\Delta\psi_m$ causes defective granulopoiesis during neutrophil differentiation from HAX1-iPS cells, similar to the process observed in SCN patients with *HAX1* gene deficiency.

Lentiviral transduction of HAX1 cDNA improves maturation arrest and apoptotic predisposition of HAX1-iPS cells

Because most *HAX1* gene mutations in SCN patients are nonsense mutations resulting in a premature stop codon and protein truncation,[23] loss of the HAX1 protein is believed to cause severe neutropenia. To uncover the pathophysiological hallmarks of this disease, we performed lentiviral transduction of *HAX1* cDNA into HAX1-iPS cells.

We constructed lentiviral vectors that expressed *HAX1* cDNA and EGFP as a marker gene (pCSII-EF-IEGFP; EGFP

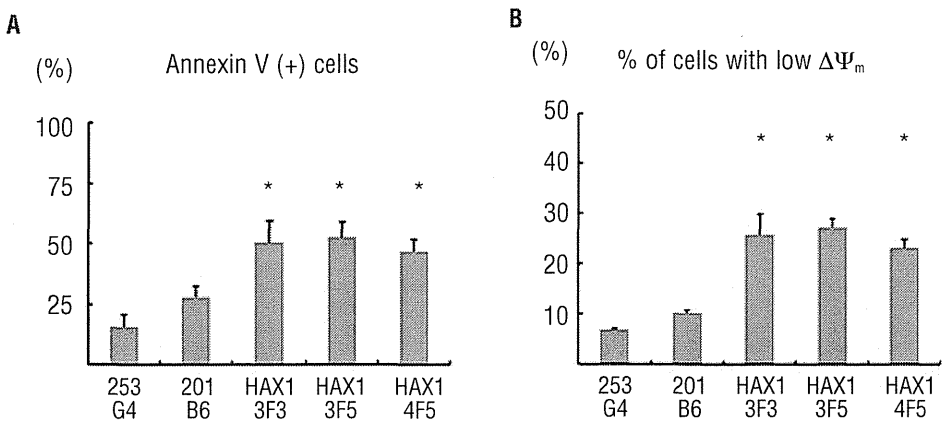

Figure 3. Neutrophils derived from HAX1-iPS cells are predisposed to undergo apoptosis due to their reduced $\Delta\psi$m. Annexin V assay (A) and mitochondrial membrane potential assay (B) of iPS cell-derived cells on Day 26 of neutrophil differentiation using flow cytometry. Cells gated on human $CD45^+$ were analyzed (n = 3; bars represent SDs; *$P<0.05$ to control iPS cells).

only, pCSII-EF-HAX1-IEGFP; HAX1 cDNA and EGFP) (Figure 4A). Efficient transduction of HAX1-iPS cells with these lentiviral vectors (HAX1 3F5+GFP; HAX1 3F5 transduced with pCSII-EF-IEGFP, HAX1 3F5+HAX1; HAX1 3F5 transduced with pCSII-EF-HAX1-IEGFP) was confirmed by a significant increase in HAX1 protein by Western blotting analysis (Figure 4B).

We then differentiated these lentiviral-transduced iPS cells into neutrophils, and examined whether defective granulopoiesis and apoptotic predisposition could be reversed. Morphologically, cells derived from HAX1 3F5+HAX1 showed a higher proportion of mature neutrophils than cells derived from HAX1 3F5+GFP and HAX1 3F5 (Figure 5A and B). Flow cytometric analysis revealed that the proportion of $CD34^+$ cells was significantly lower in the cells derived from HAX1 3F5+HAX1 than HAX1 3F5+GFP and HAX1 3F5 (Figure 5C). Immunocytochemical analysis for lactoferrin and gelatinase showed that the proportion of these granule-positive cells in generated blood cells was significantly higher in HAX 3F5+HAX1 than in HAX13F5+GFP and HAX1 3F5 (Figure 5D). These results indicated that *HAX1* cDNA increased the number of mature neutrophils in the neutrophil differentiation culture from HAX1-iPS cells *in vitro*. In addition, the percentage of NE-positive cells was significantly higher in cells derived from HAX1 3F5+HAX1 than in cells derived from HAX1 3F5+GFP and HAX1 3F5 (Figure 5E). Furthermore, the number of colonies derived from HAX1 3F5+HAX1 was comparable to the number derived from control cells (Figure 5F).

HAX1 3F5+HAX1-derived blood cells showed a significantly lower percentage of Annexin V-positive cells (Figure 6A) and a significantly lower percentage of cells with a low $\Delta\psi_m$ (Figure 6B) than HAX13F5+GFP and HAX1 3F5-derived blood cells. These results indicated that only *HAX1* cDNA transduction improved defective granulopoiesis and apoptotic predisposition due to low $\Delta\psi_m$ in the neutrophil differentiation culture from HAX1-iPS cells *in vitro*.

Discussion

Animal models and *in vitro* cultures consisting of cells derived from patients are often used to investigate disease pathophysiology and to develop novel therapies. Unfortunately, *Hax1* knock-out mice fail to reproduce abnormal granulopoiesis as observed in SCN patients.[10] Moreover, bone marrow cells are not an ideal experimental tool because it is difficult to obtain sufficient blood cells due to the invasiveness of the aspiration procedure. Moreover, the pathophysiological mechanisms occurring during early granulopoiesis are difficult to address in primary patient samples.

Our established culture system efficiently induced directed hematopoietic differentiation, which consisted of myeloid cells at different stages of development, from various control and patient-derived HAX1-iPS cell lines. Furthermore, this *in vitro* neutrophil differentiation system produced sufficient myeloid cells, which enabled us to perform various types of assays. In addition, flow cytom-

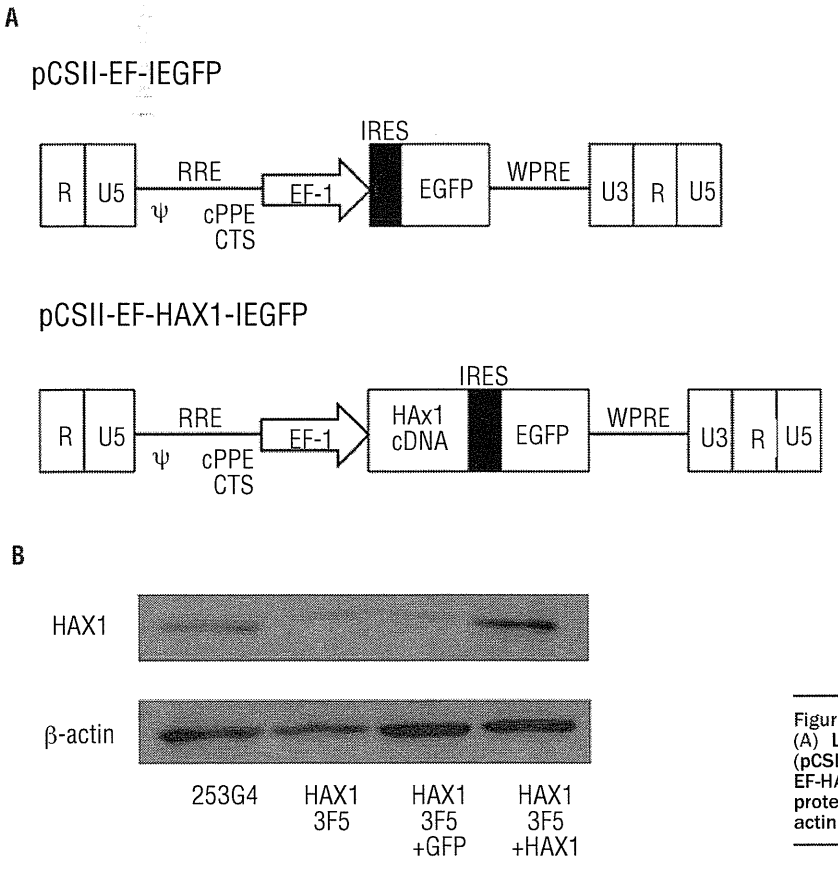

Figure 4. Lentiviral transduction of HAX1-iPS cells. (A) Lentiviral vector constructs with only EGFP (pCSII-EF-IEGFP), and *HAX1* cDNA and EGFP (pCSII-EF-HAX1-IEGFP). (B) Western blot analysis for HAX1 protein in lentivirally-transduced HAX1-iPS cells. β-actin was used as a loading control.

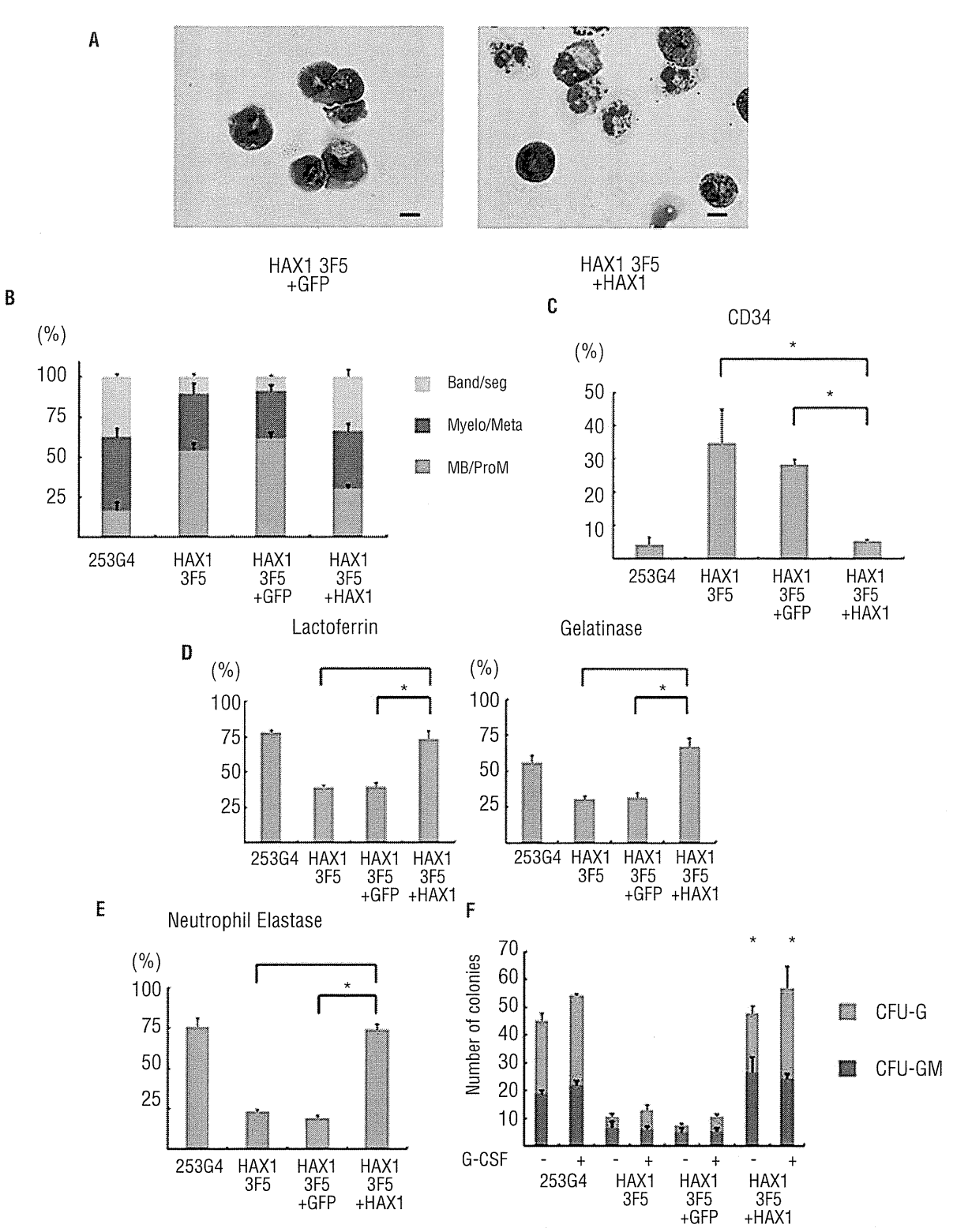

Figure 5. Lentiviral transduction of HAX1 cDNA improves maturation arrest of HAX1-iPS cells. (A) May-Giemsa staining of CD45$^+$ cells derived from HAX1 3F5+GFP and HAX1 3F5+HAX1 cells. Scale bars: 10 μm. (B) Morphological classification of CD45$^+$ cells derived from lentivirally-transduced iPS cells. (n = 3; bars represent SDs). (C) Flow cytometric analysis of CD45$^+$ cells derived from lentivirally-transduced iPS cells. Cells gated on GFP$^+$ human CD45$^+$ DAPI$^-$ were analyzed (n = 3; bars represent SDs; *P<0.05). (D) Immunocytochemical analysis of CD45$^+$ cells derived from lentivirally-transduced iPS cells (n = 3; bars represent SDs; *P<0.05). (E) NE staining of CD45$^+$ cells derived from lentivirally-transduced iPS cells (n = 3; bars represent SDs; *P<0.05). (F) Colony-forming assay of lentivirally-transduced cells derived from iPS cells. The number of colonies derived from 1×10^4 cells is indicated (n = 3; bars represent SD; *P<0.05 compared to HAX1 3F5 and HAX1 3F5+GFP). (A-E) Live CD45$^+$ cells derived from lentivirally-transduced iPS cells on Day 26 of neutrophil differentiation were analyzed. Dead cells and CD45$^-$ cells were depleted using an autoMACS Pro separator (see *Methods*).

etry, a colony-forming assay, and cytostaining of HAX1-iPS cell-derived blood cells quantitatively demonstrated maturation arrest at the progenitor level and apoptotic predisposition due to low $\Delta\psi_m$ resulting in defective granulopoiesis, which were typically observed in SCN patients with *HAX1* gene deficiency. Thus, our culture system may serve as a novel experimental model and a platform for high-throughput screening of drugs for neutropenia in SCN with *HAX1* gene deficiency.

A colony-forming assay showed that the response to G-CSF administration correlated well with the responsiveness of SCN patients to G-CSF therapy. Defective granulopoiesis was recently reported in SCN-iPS cells with a mutation in *ELANE*.[24] Our data showing defective granulopoiesis and reduced response to G-CSF administration are generally consistent with this report. The slight differences in CFU-G/GM colony-forming potential between this previous study and the current study might be due to differences in the causative gene (*HAX1* or *ELANE*) or the culture system used for neutrophil differentiation, and/or to variation in the differentiation capabilities of the clones.

In our serum and feeder-free monolayer culture system, human ES and iPS cells differentiate into hematopoietic and endothelial cells via common KDR$^+$CD34$^+$ hemoangiogenic progenitors, which exist during early embryogenesis.[18] Therefore, emergence of abnormal granulopoiesis in this system suggests that disease onset might occur at early hematopoietic stage (yolk sac or fetal liver), which would have never been addressed with patient samples.

We also showed that *HAX1* cDNA transduction could reverse disease-related phenotypes such as abnormal granulopoiesis and apoptotic predisposition. Although little is known about the pathophysiology of SCN with *HAX1* gene deficiency, these results clearly indicated that a loss in HAX1 protein might be the primary cause of neutropenia. These results also indicated the possibility of using patient-derived iPS cells for gene therapy; however, there are technical difficulties that would preclude these cells from being used in a clinical setting. Lentiviral vectors that randomly integrate transgenes can affect the expression of related genes, including cancer-related genes.[25-28] To overcome these problems, we are required to select clones in which transgenes are integrated 'safe harbor' sites and highly expressed without perturbation of neighboring gene expression,[29] or to take the zinc finger nuclease-mediated gene targeting approach[30-32] specifically to a predesigned safe harbor site such as the *AAVS1* locus,[33] which has previously been shown to permit stable expression of transgenes with minimal effects on nearby genes.

The pluripotency of patient-derived iPS cells enables investigation of the pathophysiology of various organ abnormalities and/or dysfunctions. Many types of inherited bone marrow failure syndrome were characterized by multisystem developmental defects that affected the heart, kidney, skeletomuscular system, and central nervous system. Among these, neurological symptoms were frequently seen in SCN patients with *HAX1* gene deficiency,[19,23,34] suggesting that a loss in HAX1 may also affect neural development. Indeed, our patient also presented for epilepsy and severe delays in motor, cognitive, and intellectual development.[19] In patient-derived cells, $\Delta\psi_m$ was not reduced in undifferentiated iPS cells but was reduced in differentiated neutrophils. No marked abnormalities in teratoma formation by HAX1-iPS cells were observed. These results are partially consistent with the fact that SCN patients with a *HAX1* gene deficiency have only neutropenia and neurological symptoms, despite *HAX1* being a ubiquitously expressed gene.[6] Because some of these neurological symptoms cannot be reproduced in the currently available mouse model,[10] additional studies will be necessary to address the effects of *HAX1* on neural development by directed culture models of patient-derived iPS cells.

In conclusion, patient-derived iPS cell-derived myeloid cells were similar in disease presentation to SCN patients with *HAX1* gene deficiency, which could be reversed by gene correction in a novel *in vitro* neutrophil differentiation system. This culture system will serve as a new tool to facilitate disease modeling and drug screening for congenital neutrophil disorders.

Acknowledgments

The authors would like to thank Dr. Norio Nakatsuji for providing the human ES cell line KhES-1, Dr. Shinya Yamanaka for providing human iPS cell lines 201B6 and 253G4, and Dr. Hiroyuki Miyoshi for providing pCSII-EF-MCS. We are grate-

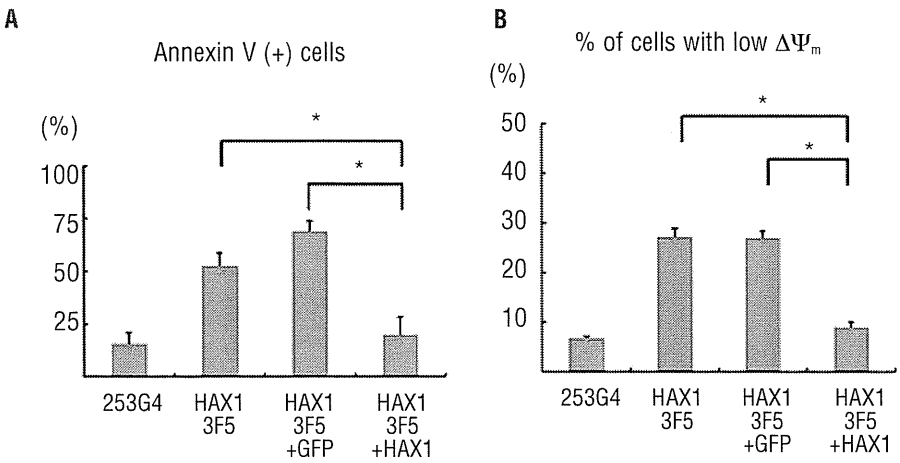

Figure 6. Lentiviral transduction of *HAX1* cDNA prevents HAX1-iPS cells being predisposed to undergo apoptosis. Annexin V assay (A) and mitochondrial membrane potential assay (B) of lentivirally-transduced iPS cell-derived cells on Day 26 of neutrophil differentiation. Cells gated on GFP$^+$ human CD45$^+$ were analyzed (n = 3; bars represent SDs; *P<0.05).

ful to Kyowa Hakko Kirin for providing TPO and G-CSF. We also thank the Center for Anatomical Studies, Kyoto University Graduate School of Medicine, for immunocytochemical analysis. Funding was provided by grants from the Ministry of Health, Labour and Welfare to KW, TN, and TH, a grant from the Ministry of Education, Culture, Sports, Science and Technology (MEXT) to KW, TN, and TH, grants from the Leading Project of MEXT to TN, a grant from Funding Program for World-Leading Innovative Research and Development on Science and Technology (FIRST Program) of Japan Society for the Promotion of Science (JSPS) to TN, grants from the SENSHIN Medical Research Foundation to IK, and grants from the Fujiwara Memorial Foundation to TM. This work was also supported by the Global COE Program "Center for Frontier Medicine" from MEXT, Japan.

Authorship and Disclosures

Information on authorship, contributions, and financial & other disclosures was provided by the authors and is available with the online version of this article at www.haematologica.org.

References

1. Welte K, Zeidler C, Dale DC. Severe congenital neutropenia. Semin Hematol. 2006;43(3):189-95.
2. Skokowa J, Germeshausen M, Zeidler C, Welte K. Severe congenital neutropenia: inheritance and pathophysiology. Curr Opin Hematol. 2007;14(1):22-8.
3. Dale DC, Person RE, Bolyard AA, Aprikyan AG, Bos C, Bonilla MA, et al. Mutations in the gene encoding neutrophil elastase in congenital and cyclic neutropenia. Blood. 2000;96(7):2317-22.
4. Kostmann R. Infantile genetic agranulocytosis; agranulocytosis infantilis hereditaria. Acta Paediatr Suppl. 1956;45(Suppl 105):1-78.
5. Klein C, Grudzien M, Appaswamy G, Germeshausen M, Sandrock I, Schaffer AA, et al. HAX1 deficiency causes autosomal recessive severe congenital neutropenia (Kostmann disease). Nat Genet. 2007;39 (1):86-92.
6. Suzuki Y, Demoliere C, Kitamura D, Takeshita H, Deuschle U, Watanabe T. HAX-1, a novel intracellular protein, localized on mitochondria, directly associates with HS1, a substrate of Src family tyrosine kinases. J Immunol. 1997;158(6):2736-44.
7. Sharp TV, Wang HW, Koumi A, Hollyman D, Endo Y, Ye H, et al. K15 protein of Kaposi's sarcoma-associated herpesvirus is latently expressed and binds to HAX-1, a protein with antiapoptotic function. J Virol. 2002;76(2):802-16.
8. Freedman MH, Bonilla MA, Fier C, Bolyard AA, Scarlata D, Boxer LA, et al. Myelodysplasia syndrome and acute myeloid leukemia in patients with congenital neutropenia receiving G-CSF therapy. Blood. 2000;96(2):429-36.
9. Rosenberg PS, Zeidler C, Bolyard AA, Alter BP, Bonilla MA, Boxer LA, et al. Stable long-term risk of leukaemia in patients with severe congenital neutropenia maintained on G-CSF therapy. Br J Haematol. 2010;150(2):196-9.
10. Chao JR, Parganas E, Boyd K, Hong CY, Opferman JT, Ihle JN. Hax1-mediated processing of HtrA2 by Parl allows survival of lymphocytes and neurons. Nature. 2008;452(7183):98-102.
11. Takahashi K, Yamanaka S. Induction of pluripotent stem cells from mouse embryonic and adult fibroblast cultures by defined factors. Cell. 2006;126(4):663-76.
12. Takahashi K, Tanabe K, Ohnuki M, Narita M, Ichisaka T, Tomoda K, et al. Induction of pluripotent stem cells from adult human fibroblasts by defined factors. Cell. 2007;131(5):861-72.
13. Meissner A, Wernig M, Jaenisch R. Direct reprogramming of genetically unmodified fibroblasts into pluripotent stem cells. Nat Biotechnol. 2007;25(10):1177-81.
14. Okita K, Ichisaka T, Yamanaka S. Generation of germline-competent induced pluripotent stem cells. Nature. 2007; 448(7151):313-7.
15. Park IH, Zhao R, West JA, Yabuuchi A, Huo H, Ince TA, et al. Reprogramming of human somatic cells to pluripotency with defined factors. Nature. 2008;451(7175): 141-6.
16. Yu J, Vodyanik MA, Smuga-Otto K, Antosiewicz-Bourget J, Frane JL, Tian S, et al. Induced pluripotent stem cell lines derived from human somatic cells. Science. 2007;318(5858):1917-20.
17. Morishima T, Watanabe K, Niwa A, Fujino H, Matsubara H, Adachi S, et al. Neutrophil differentiation from human-induced pluripotent stem cells. J Cell Physiol. 2011;226(5):1283-91.
18. Niwa A, Heike T, Umeda K, Oshima K, Kato I, Sakai H, et al. A novel serum-free monolayer culture for orderly hematopoietic differentiation of human pluripotent cells via mesodermal progenitors. PLoS One. 2011;6(7):e22261.
19. Matsubara K, Imai K, Okada S, Miki M, Ishikawa N, Tsumura M, et al. Severe developmental delay and epilepsy in a Japanese patient with severe congenital neutropenia due to HAX1 deficiency. Haematologica. 2007;92(12):e123-5.
20. Skokowa J, Fobiwe JP, Dan L, Thakur BK, Welte K. Neutrophil elastase is severely down-regulated in severe congenital neutropenia independent of ELA2 or HAX1 mutations but dependent on LEF-1. Blood. 2009;114(14):3044-51.
21. Kobayashi M, Yumiba C, Kawaguchi Y, Tanaka Y, Ueda K, Komazawa Y, et al. Abnormal responses of myeloid progenitor cells to recombinant human colony-stimulating factors in congenital neutropenia. Blood. 1990;75(11):2143-9.
22. Konishi N, Kobayashi M, Miyagawa S, Sato T, Katoh O, Ueda K. Defective proliferation of primitive myeloid progenitor cells in patients with severe congenital neutropenia. Blood. 1999;94(12):4077-83.
23. Germeshausen M, Grudzien M, Zeidler C, Abdollahpour H, Yetgin S, Rezaei N, et al. Novel HAX1 mutations in patients with severe congenital neutropenia reveal isoform-dependent genotype-phenotype associations. Blood. 2008;111(10):4954-7.
24. Hiramoto T, Ebihara Y, Mizoguchi Y, Nakamura K, Yamaguchi K, Ueno K, et al. Wnt3a stimulates maturation of impaired neutrophils developed from severe congenital neutropenia patient-derived pluripotent stem cells. Proc Natl Acad Sci USA. 2013; 110(8):3023-8.
25. Hacein-Bey-Abina S, Von Kalle C, Schmidt M, McCormack MP, Wulffraat N, Leboulch P, et al. LMO2-associated clonal T cell proliferation in two patients after gene therapy for SCID-X1. Science. 2003;302(5644):415-9.
26. Ott MG, Schmidt M, Schwarzwaelder K, Stein S, Siler U, Koehl U, et al. Correction of X-linked chronic granulomatous disease by gene therapy, augmented by insertional activation of MDS1-EVI1, PRDM16 or SETBP1. Nat Med. 2006;12(4):401-9.
27. Howe SJ, Mansour MR, Schwarzwaelder K, Bartholomae C, Hubank M, Kempski H, et al. Insertional mutagenesis combined with acquired somatic mutations causes leukemogenesis following gene therapy of SCID-X1 patients. J Clin Invest. 2008; 118(9):3143-50.
28. Cavazzana-Calvo M, Payen E, Negre O, Wang G, Hehir K, Fusil F, et al. Transfusion independence and HMGA2 activation after gene therapy of human beta-thalassaemia. Nature. 2010;467(7313):318-22.
29. Papapetrou EP, Lee G, Malani N, Setty M, Riviere I, Tirunagari LM, et al. Genomic safe harbors permit high beta-globin transgene expression in thalassemia induced pluripotent stem cells. Nat Biotechnol. 2011;29 (1):73-8.
30. Zou J, Sweeney CL, Chou BK, Choi U, Pan J, Wang H, et al. Oxidase-deficient neutrophils from X-linked chronic granulomatous disease iPS cells: functional correction by zinc finger nuclease-mediated safe harbor targeting. Blood. 2011;117(21):5561-72.
31. DeKelver RC, Choi VM, Moehle EA, Paschon DE, Hockemeyer D, Meijsing SH, et al. Functional genomics, proteomics, and regulatory DNA analysis in isogenic settings using zinc finger nuclease-driven transgenesis into a safe harbor locus in the human genome. Genome Res. 2010;20(8): 1133-42.
32. Hockemeyer D, Soldner F, Beard C, Gao Q, Mitalipova M, DeKelver RC, et al. Efficient targeting of expressed and silent genes in human ESCs and iPSCs using zinc-finger nucleases. Nat Biotechnol. 2009;27(9):851-7.
33. Henckaerts E, Dutheil N, Zeltner N, Kattman S, Kohlbrenner E, Ward P, et al. Site-specific integration of adeno-associated virus involves partial duplication of the target locus. Proc Natl Acad Sci USA. 2009;106(18):7571-6.
34. Ishikawa N, Okada S, Miki M, Shirao K, Kihara H, Tsumura M, et al. Neurodevelopmental abnormalities associated with severe congenital neutropenia due to the R86X mutation in the HAX1 gene. J Med Genet. 2008;45(12):802-7.

e-Blood

PLATELETS AND THROMBOPOIESIS

Platelet diameters in inherited thrombocytopenias: analysis of 376 patients with all known disorders

Patrizia Noris,[1] Ginevra Biino,[2] Alessandro Pecci,[1] Elisa Civaschi,[1] Anna Savoia,[3,4] Marco Seri,[5] Federica Melazzini,[1] Giuseppe Loffredo,[6] Giovanna Russo,[7] Valeria Bozzi,[1] Lucia Dora Notarangelo,[8] Paolo Gresele,[9] Paula G. Heller,[10] Nuria Pujol-Moix,[11] Shinji Kunishima,[12] Marco Cattaneo,[13] James Bussel,[14] Erica De Candia,[15] Claudia Cagioni,[1] Ugo Ramenghi,[16] Serena Barozzi,[1] Fabrizio Fabris,[17] and Carlo L. Balduini[1]

[1]Department of Internal Medicine, University of Pavia-Istituto Di Ricovero e Cura a Carattere Scientifico Policlinico San Matteo Foundation, Pavia, Italy; [2]Institute of Molecular Genetics, National Research Council of Italy, Pavia, Italy; [3]Department of Medical Sciences, University of Trieste, Trieste, Italy; [4]Institute for Maternal and Child Health–Istituto Di Ricovero e Cura a Carattere Scientifico Burlo Garofolo, Trieste, Italy; [5]Genetica Medica, Dipartimento di Scienze Mediche Chirurgiche, Policlinico Sant'Orsola-Malpighi, University of Bologna, Bologna, Italy; [6]Department of Oncology, Azienda "Santobono-Pausilipon," Pausilipon Hospital, Naples, Italy; [7]Division of Pediatric Hematology/Oncology, University of Catania, Catania, Italy; [8]Oncology-Haematology and Bone Marrow Transplantation Unit, Ospedale dei Bambini, Spedali Civili, Brescia, Italy; [9]Department of Medicine, Section of Internal and Cardiovascular Medicine, University of Perugia, Perugia, Italy; [10]Department of Hematology Research, Instituto de Investigaciones Médicas Alfredo Lanari, National Scientific and Technical Research Council, University of Buenos Aires, Buenos Aires, Argentina; [11]Universitat Autònoma de Barcelona, Institut de Recerca Biomèdica Sant Pau, Barcelona, Spain; [12]Department of Advanced Diagnosis, Clinical Research Center, National Hospital Organization Nagoya Medical Center, Nagoya, Japan; [13]Medicina III Ospedale San Paolo, Dipartimento di Scienza della Salute, Università degli Studi di Milano, Milan, Italy; [14]Weill Medical College of Cornell University, New York, NY; [15]Servizio Malattie Emorragiche e Trombotiche, Istituto di Medicina Interna e Geriatria, Policlinico Agostino Gemelli, Università Cattolica del Sacro Cuore, Rome, Italy; [16]Hematology Unit, Pediatric Department, University of Torino, Torino, Italy; and [17]Department of Medicine; University of Padova Medical School, Padova, Italy

Key Points

- Measurement of platelet diameters in 376 patients resulted in a new classification of inherited thrombocytopenias based on platelet size.
- Measurement of platelet diameters is a useful tool for differential diagnosis of inherited thrombocytopenias.

Abnormalities of platelet size are one of the distinguishing features of inherited thrombocytopenias (ITs), and evaluation of blood films is recommended as an essential step for differential diagnosis of these disorders. Nevertheless, what we presently know about this subject is derived mainly from anecdotal evidence. To improve knowledge in this field, we evaluated platelet size on blood films obtained from 376 patients with all 19 forms of IT identified so far and found that these conditions differ not only in mean platelet diameter, but also in platelet diameter distribution width and the percentage of platelets with increased or reduced diameters. On the basis of these findings, we propose a new classification of ITs according to platelet size. It distinguishes forms with giant platelets, with large platelets, with normal or slightly increased platelet size, and with normal or slightly decreased platelet size. We also measured platelet diameters in 87 patients with immune thrombocytopenia and identified cutoff values for mean platelet diameter and the percentage of platelets with increased or reduced size that have good diagnostic accuracy in differentiating ITs with giant platelets and with normal or slightly decreased platelet size from immune thrombocytopenia and all other forms of IT. (*Blood.* 2014;124(6):e4-e10)

Introduction

Until recently, inherited thrombocytopenias (ITs) were considered exceedingly rare, and only a few forms were known. The advancement of knowledge about these disorders in recent years identified several new forms, which were found to be much more frequent than the diseases known up to the end of the last century. Better knowledge of ITs changed our view of their clinical characteristics and showed that thrombocytopenia is mild in most cases and is often identified for the first time in adult life.[1] If no other family members are known to be thrombocytopenic, the patients are at risk of being misdiagnosed with immune thrombocytopenic purpura (ITP). In fact, a number of patients with ITs receiving undue treatments for a wrong diagnosis of ITP have been reported.[1]

Early diagnosis of ITs is important not only to avoid unnecessary treatments but also to define both prognosis and therapy for patients. In fact, some genetic defects that cause congenital thrombocytopenia expose patients to the risk of developing diseases that are fatal if not treated appropriately. For instance, mutations of *RUNX1* and *ANKRD26*, which are responsible for familial platelet disorder (FPD) with predisposition to acute myeloid leukemia (AML) and *ANKRD26*-related thrombocytopenia (*ANKRD26*-RT), respectively, greatly increase the risk of myeloid malignancies, whereas mutations of *MPL*, which is responsible for congenital amegakaryocytic thrombocytopenia (CAMT), always evolves into a bone marrow aplasia before adulthood.[2] Thus, recognizing these disorders allow

Submitted March 21, 2014; accepted June 24, 2014. Prepublished online as *Blood* First Edition paper, July 2, 2014; DOI 10.1182/blood-2014-03-564328.

The publication costs of this article were defrayed in part by page charge payment. Therefore, and solely to indicate this fact, this article is hereby marked "advertisement" in accordance with 18 USC section 1734.

Table 1. Number of investigated participants and their main characteristics

Disorder	Abbreviation in main text	Phenotype MIM number	No. of investigated participants	Age (y)				Platelet count × 10^9/L	
				Mean	SD	F	M	Mean	SD
Bernard-Soulier syndrome	BSS	231200	127	31	18.8	69	58	82	33.7
Biallelic BSS	bBSS		13	26	16.8	8	5	41	34.6
Monoallelic BSS	mBSS		114	32	19	61	53	87	30.2
MYH9-related disease	*MYH9*-RD	600208	125	33	19.3	59	66	35	25.9
MYH9-RD tail mutation	t*MYH9*-RD		100	35	19.9	48	52	39	26
MYH9-RD head mutation	h*MYH9*-RD		25	26	15.2	11	14	19	18.6
ANKRD26-related thrombocytopenia	*ANKRD26*-RT	188000	58	40	20.7	27	31	43	28.4
A*CTN1*-related thrombocytopenia	*ACTN1*-RT	615193	20	36	21.5	14	6	87	31.7
Wiskott-Aldrich syndrome/ X-linked thrombocytopenia	WAS/XLT	301000/ 313900	9	20	16.7	0	9	61	64.7
Congenital amegakaryocytic thrombocytopenia	CAMT	604498	5	4	2.7	2	3	13	4.7
Gray platelet syndrome	GPS	139090	5	37	31.5	0	5	55	21.3
ITGA2B/ITGB3-related thrombocytopenia	*ITGA2B/B3*-RT	187800	5	28	15.9	5	0	106	44.9
TUBB1-related thrombocytopenia	*TUBB1*-RT	613112	5	20	12.6	2	3	82	44.7
Familial platelet disorder and predisposition to acute myeloid leukemia	FPD-AML	601399	4	20	13.5	2	2	103	35.9
CYCS-related thrombocytopenia	*CYCS*-RT	612004	3	32	14	1	2	104	61.7
FLNA-related thrombocytopenia	*FLNA*-RT		2	16	20.5	2	0	34	12.7
Thrombocytopenia Paris-Trousseau	TCPT	188025	2	0.2	0.06	1	1	49	9.9
GFI1B-related thrombocytopenia	*GFI1B*-RT	187900	2	15	0	1	1	97	24.7
Congenital thrombocytopenia with radioulnar synostosis	CTRUS	605432	1	10		0	1	30	
von Willebrand disease platelet-type	VWDP	177820	1	30		1	0	130	
Thrombocytopenia with absent radii	TAR	274000	1	6		1	0	19	
X-linked thrombocytopenia with thalassemia	XLTT	314050	1	8		0	1	75	
ITP			87	38	26.4	50	37	48	31.1
Controls			55	37	17	29	26	257	52.3

F, female; M, male; MIM, Mammalian Inheritance in Man.

physicians to tailor follow-up to the specific risk profiles of each patient and to be ready to perform bone marrow transplantation as soon as required. It has also been shown that the thrombopoietin mimetic eltrombopag increases platelet count in most patients with *MYH9*-related disease (*MYH9*-RD).[3] Thus, making the correct diagnosis allows physicians to use eltrombopag instead of platelet transfusions to prepare patients for surgery or invasive procedures.[4] Making a definite diagnosis can therefore improve the management of patients with ITs.

Platelet size is unanimously recognized as one of the most important parameters for determining the genetic origin of thrombocytopenia and guiding the differential diagnosis of the various specific conditions, in that abnormalities of platelet dimensions have been described in the majority of ITs. Nevertheless, using platelet size for differentiation is poorly defined for two main reasons. First, the rarity of ITs makes it difficult to directly compare platelet size in patients with different disorders. Second, both impedentiometric and optical cell counters systematically underestimate platelet volume (as well as platelet count) in inherited macrothrombocytopenias because of their inability to recognize very large platelets.[5] Moreover, instruments that operate on different principles induce variability into the measurement of platelet volume in patients with nonmacrocytic thrombocytopenias as well as in healthy participants, thus making it difficult to compare values obtained in different centers.[6] As a consequence, what we presently know about this subject is derived mainly from case reports, series of patients with one form of IT, and two small studies that directly compared platelet size in some of the known ITs.[5,7]

To advance knowledge in this field (taking into account the present limitations of cell counters), we performed a collaborative study to measure platelet size by image analysis of peripheral blood smears obtained from patients affected by all 19 forms of IT currently known.

Patients and methods

Patients

In all, 376 patients with 19 forms of IT, 87 patients with ITP, and 55 healthy participants have been studied. IT patients were from 10 different countries (Argentina, Germany, Greece, Holland, Italy, Japan, United Kingdom, United States, Spain, and Switzerland), although the vast majority (80%) were from Italy. All ITP patients and control participants were Italian.

The main characteristics of the investigated participants are reported in Table 1. Diagnosis of ITs was always confirmed by the identification of causative mutations. Since genotype/phenotype studies in *MYH9*-RD revealed that clinical and laboratory abnormalities are more severe in patients with mutations in the head domain of the molecule than in those with mutations in the tail domain,[8,9] these 2 categories of patients were analyzed separately. Concerning Bernard-Soulier syndrome (BSS), we classified as biallelic BSS (bBSS) those patients with homozygous or double heterozygous mutations of GPIbα, GPIbβ, or GPIX, who presented with the classical form characterized by thrombocytopenia and severe platelet dysfunction. Patients with monoallelic mutations presenting with thrombocytopenia were classified as monoallelic BSS (mBSS).[2] Of note, 103 of 117 patients with mBSS had the p.Ala156Val substitution in GPIbα (Bolzano mutation), which is frequent in the Italian population.[10]

Table 2. Characteristics of platelet diameters in investigated participants

	MPD (μm)					PDDW (μm)		PDLCR (%)		PDSCR (%)	
Characteristic	Mean	95% CI	2.5th-97.5th	2.5th 95% CI	97.5th 95% CI	Mean	95% CI	Mean	95% CI	Mean	95% CI
MYH9-RD	4.51	4.2 to 4.8	2.3-8.1	2.2 to 2.3	7.8 to 8.5	5.9	5.6 to 6.2	58.3	54.8 to 61.8	0.5	0.2 to 0.8
h*MYH9*-RD	5.64	4.8 to 6.4	2.7-10.4	2.4 to 2.9	9.5 to 11.4	7.8	6.9 to 8.7	75.3	66.2 to 84.4	0.1	0 to 0.2
t*MYH9*-RD	4.28	4 to 4.6	2.1-7.6	2.1 to 2.2	7.3 to 7.8	5.4	5.1 to 5.7	54	50.7 to 57.3	0.6	0.2 to 1
TUBB1-RT	3.91	2.8 to 5.1	2.1-7.2	1.9 to 2.2	5.9 to 8.6	5.2	3.5 to 6.8	43.1	20.3 to 65.9	0	
GPS	3.76	2.7 to 4.8	2-7.2	1.8 to 2.2	6.6 to 7.9	5.2	4.2 to 6.2	36.5	22.5 to 50.6	0.4	−0.6 to 1.4
FLNA-RT	3.75	2.2 to 5.3	2.1-6.4	1.6 to 2.6	5.5 to 7.4	4.3	1.2 to 7.4	38.3	0.3 to 76.2	0.4	−4.9 to 5.8
GFI1b-RT	3.59	2.2 to 5	1.9-5.8	1.9 to 1.9	5.3 to 6.4	3.9	0.2 to 7.7	34.8	−17.5 to 87.1	1.2	−1.9 to 4.3
BSS	3.44	3.3 to 3.6	2-5.6	1.9 to 2	5.4 to 5.8	3.6	3.5 to 3.8	29.6	26.2 to 33	1.5	0.9 to 2.2
bBSS	4.24	3.7 to 4.8	2.5-6.6	2.3 to 2.7	6.2 to 7	4.1	3.7 to 4.4	58.1	48 to 68.2	0.1	−0.1 to 0.2
mBSS	3.39	3.2 to 3.6	1.9-5.5	1.8 to 2	5.4 to 5.7	3.6	3.5 to 3.8	27.3	24 to 30.6	1.8	1 to 2.5
ITGA2B/ITGB3-RT	3.39	2.5 to 4.2	2-5.7	1.6 to 2.4	4.7 to 6.7	3.7	2.6 to 4.7	23.9	5.8 to 41.9	1.2	−1 to 3.5
ACTN1-RT	3.36	2.9 to 3.8	1.8-5.8	1.7 to 1.9	5.5 to 6.2	4.1	3.8 to 4.4	25.5	19.4 to 31.5	1.6	0.6 to 2.6
FPD-AML	3.18	2.2 to 4.2	1.6-5.6	1.4 to 1.8	4.9 to 6.2	3.9	3.1 to 4.8	18.6	5.3 to 31.9	3.1	−0.9 to 7.1
TCPT	3.15	1.9 to 4.4	1.7-5.5	1.4 to 2.1	4 to 7.1	3.8	−4.4 to 12.0	24.6	−225.1 to 274.2	1.8	−8.6 to 12.3
XLTT	3.02	0.9 to 5.1	1.3-5.8	1.2 to 1.6	5.2 to 6.3	4.5		16.3		5.1	
ANKRD26-RT	2.93	2.7 to 3.1	1.8-4.8	1.7 to 1.9	4.6 to 5.1	3.1	2.8 to 3.3	12.8	9.3 to 16.2	1.6	1 to 2.1
CTRUS	2.79	1.6 to 3.9	1.8-4.3	1.7 to 1.9	3.8 to 5.3	2.5		3.5		0	
VWDP	2.74	1.6 to 3.9	1.7-4.4	1.4 to 1.9	3.7 to 5.1	2.7		3.3		1.1	
TAR	2.35	1.3 to 3.4	1.4-3.4	1.4 to 1.6	3.1 to 4.4	2		0.8		6.3	
CAMT	2.32	1.8 to 2.9	1.3-4	0.9 to 1.8	3.1 to 5	2.7	1.8 to 3.5	6.4	−9.4 to 22.2	18.9	−5.2 to 42.9
CYCS-RT	2.28	1.5 to 3.1	1.2-4.4	0.8 to 1.6	3.3 to 5.4	3.1	0.9 to 5.7	4.3	−4 to 12.6	18.8	−19.2 to 56.7
WAS/XLT	2.25	1.9 to 2.6	1.4-3.8	1.2 to 1.5	3.5 to 4.1	2.4	2.2 to 2.6	2.3	−0.1 to 4.8	10.3	3.2 to 17.3
ITP	3.11	2.9 to 3.3	1.8-5.2	1.7 to 1.8	5 to 5.4	3.5	3.3 to 3.7	16.4	13.6 to 19.2	2.8	1.3 to 4.2
Controls	2.58	2.4 to 2.7	1.6-3.9	1.5 to 1.6	3.7 to 4.1	2.3	2.2 to 2.5	3.5	2.2 to 4.8	4.7	3.1 to 6.3

ITs are listed in descending order of MPD.
CI, confidence interval.

The diagnosis of ITP was made according to guidelines of the American Society of Hematology and the British Society for Haematology,[11,12] and it was confirmed by evaluating subsequent clinical evolution and response to therapy.

The institutional review board of the Istituto Di Ricovero e Cura a Carattere Scientifico Policlinico San Matteo Foundation of Pavia, Italy, approved the study protocol. The study was performed in accordance with the Declaration of Helsinki, and each center complied with local ethical rules.

Methods

Platelet count. Platelet count was measured by the cell counters available in each center. It is worth mentioning that cell counters are at risk of underestimating platelet count in macrothrombocytopenias[5] and that, therefore, it is likely that reported data overestimated the degree of thrombocytopenia in the ITs with large platelets.

Platelet diameters. Blood smears were prepared in each center from nonanticoagulated blood obtained by finger stick and were shipped to the center that measured platelet diameters (University of Pavia- Istituto Di Ricovero e Cura a Carattere Scientifico Policlinico San Matteo Foundation, Pavia, Italy). Platelet diameters were measured by optical microscopy on May-Grünwald-Giemsa–stained blood films and by software-assisted image analysis (Axiovision 4.5; Carl Zeiss, Göttingen, Germany). On average, 200 platelets were evaluated in each patient, and the maximum diameter of each platelet was recorded.[7] Platelets in clumps or those with extending pseudopodia were not considered. Technicians who measured the diameters were blinded to the patients' diagnoses.

To evaluate the possibility of measuring the percentage of large platelets (see "Statistical analysis") without the support of software-assisted image analysis, this parameter was calculated empirically by blinded operators who visually compared the diameters of platelets with those of red cells. All blood films examined by software-assisted image analysis were also evaluated by this empirical approach.

Statistical analysis

Analyzed parameters were mean platelet diameters (MPDs), platelet diameter distribution width (PDDW) as the 97.5th to 2.5th percentiles difference, platelet diameter large cell ratio (PDLCR) as the mean percentage of platelets above the 97.5th percentile of platelet diameter distribution in controls, and platelet diameter small cell ratio (PDSCR) as the mean percentage of platelets below the 2.5th percentile of platelet diameter distribution in controls. Descriptive statistics were computed as means, standard deviations, and 2.5th to 97.5th percentiles, decomposing the standard deviation into between and within components to take into account the hierarchical structure of data (platelet diameter measurements within patients). Correlation analysis was used to assess resemblance between measuring PDLCR with or without the support of software-assisted image analysis and to determine whether age has any impact on platelet size parameters. Receiver operating characteristic analysis was performed to identify optimal cutoffs of the analyzed parameters for discriminating specific forms of ITs from all other examined pathological conditions. Stata MP 11.1 along with nrocarea package for receiver operating characteristic analysis was used for computation.

Results

Table 2 reports the mean values of MPD, PDDW, PDLCR, and PDSCR measured in investigated conditions together with their 95% CIs.

MPD

Figure 1A shows MPDs measured by software-assisted image analysis in different groups of patients and controls, together with the 25th to 75th percentiles and the most extreme values. The categories of patients are reported from left to right in descending order of the medians of MPDs. Patients with *MYH9*-RD due to mutations in the head domain of *MYH9* had the highest MPD with a value of 5.64 μm. Interestingly, MPD was much lower in patients with *MYH9*-RD deriving from mutations in the tail domain of *MYH9* who had MPD similar to that measured in bBSS. *MYH9*-RD and bBSS were the only

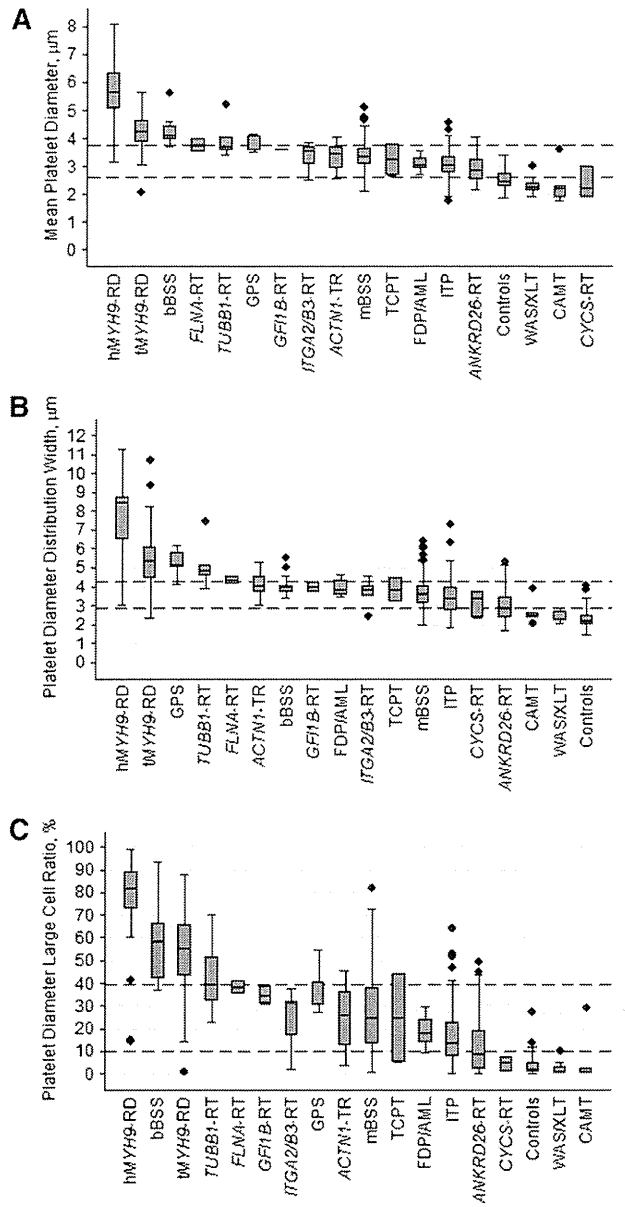

Figure 1. Platelet size parameters. (A) MPDs, (B) PDDWs and (C) PDLCRs in ITs, immune thrombocytopenia, and controls. Disorders with only 1 examined patient are not reported. Lines in the middle of the box are the medians, boxes are defined by the 25th and 75th percentiles (quartile 1 [Q1] and quartile 3 [Q3]), the ends of the whiskers are the most extreme values within Q3 + 1.5(Q3 − Q1) and Q1 − 1.5(Q3 − Q1), respectively, and dots are outliers. The dashed horizontal lines indicate the best cutoff values for distinguishing ITs with giant platelets (upper lines) and those with normal or slightly decreased platelet size (lower lines) from the other forms of ITs and immune thrombocytopenia.

ITs with MPDs larger than 4 µm. Results for ITP patients are located to the left of those for healthy participants, and only Wiskott-Aldrich syndrome (WAS)/X-linked thrombocytopenia (XLT), CAMT, and *CYCS*-related thrombocytopenia (*CYCS*-RT) are to the right results for controls. WAS and XLT derive from mutations in the WAS gene, but they are often considered separate entities because of differences in their clinical phenotypes. Moreover, it has been reported that splenectomy increased platelet size as well as platelet count of affected patients.[13] On this basis, we analyzed patients with WAS and XLT separately, separating splenectomized patients from non-splenectomized ones. Although MPDs were slightly larger in XLT than in WAS as well in splenectomized patients versus non-splenectomized patients, all these differences were subtle and far from being statistically significant. Thus, for the purposes of this study, we considered all patients with WAS mutations as belonging to a single category.

Because a mild increase (about 5%) in platelet volume has been observed in patients older than age 60 years vs those younger than age 18 years,[14] we searched for correlation between age and MPD both in the entire population of investigated patients and in the disorders with more than 8 patients. No significant correlation has been found (data not shown), suggesting that age differences in different categories of investigated patients did not significantly interfere with the results of platelet diameter measurement.

PDDW

PDDWs in different conditions are reported in Figure 1B. Comparison of MPDs in Figure 1A-B indicates that PDDWs and MPDs are largely related values, in that PDDWs increase with increasing MPDs both in ITs and ITP. The lowest value of PDDW has been observed in controls.

PDLCR

As shown in Figure 1C, the analysis of the percentage of large platelets in different conditions provided interesting results. PDLCR, defined as the proportion of platelets with diameters larger than the 97.5th percentile of MPD in healthy participants (>3.9 µm) was above 5% in the vast majority of ITs as well as in ITP. In particular, 11 and 3 ITs had median PDLCRs larger than 20% and 50%, respectively. The increase in large platelets was clearly related to the increase in platelet diameters, but differences with respect to controls were larger for PDLCRs than MPDs, although wide variations of PDLCRs were observed within patients with the same disorder. Of note, low values of PDLCRs were observed in ITs with the smallest MPDs.

Empirical evaluation by a blinded operator of the percentages of platelets larger than 3.9 µm (half the diameter of red cells) in patients and controls showed excellent correlation with the values obtained by software-assisted image analysis (Pearson's $r = 0.95$; $P < .0001$).

PDSCR

Concerning PDSCR, defined as the percentage of platelets smaller than the 2.5th percentile of MPD in healthy participants (<1.6 µm), the highest values have been observed in *CYCS*-RT, CAMT, and WAS/XLT, with values of 18.8%, 18.9%, and 10.3%, respectively (Figure 2).

Platelet diameters for differential diagnosis between ITs and ITP

Given the results of the descriptive analysis, we wondered whether platelet diameters could play a role in differentiating ITs from ITP. Evaluation of the data reported in Table 2 and in Figures 1-2 indicates that MPD, PDDW, PDLCR, and PDSCR in many ITs were largely overlapping with those observed in ITP. Notable exceptions were represented by a head mutation in *MYH9*-RD (h*MYH9*-RD), a tail mutation in *MYH9*-RD (t*MYH9*-RD), and bBSS, which had values of MPDs, PDDWs, and PDLCRs above and rather well separated from those measured in ITP. Conversely, the values of MPDs, PDDWs, and PDLCR in WAS/XLT, CAMT, and *CYCS*-RT were below those measured in ITP. These ITs were also characterized by PDLCRs higher than those in ITP. Thus, we searched for the best cutoff values for distinguishing these conditions and measured their diagnostic accuracy. Table 3 reports the results of these analyses of ITs with large platelets.

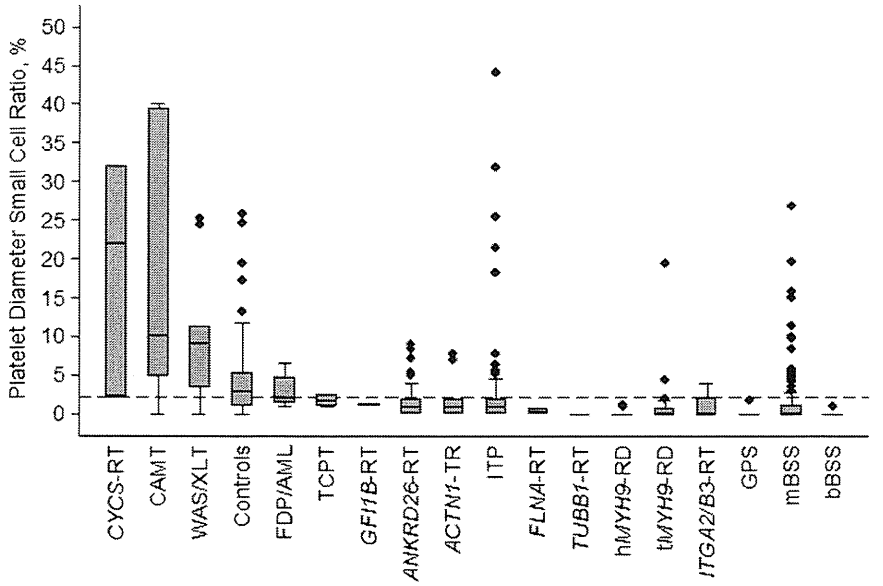

Figure 2. PDSCRs in ITs, immune thrombocytopenia, and controls. Disorders with only 1 examined patient are not reported. Line in the middle of the box is the median, box is defined by the 25th and 75th percentiles (Q1 and Q3), and the ends of the whiskers are the most extreme values within Q3 + 1.5(Q3 − Q1) and Q1 − 1.5(Q3 − Q1), respectively. The dashed horizontal line indicates the best cutoff value for distinguishing ITs with normal or slightly decreased platelet size from the other forms of ITs and immune thrombocytopenia.

An MPD larger than 3.74 μm and a PDLCR higher than 39.8% had good sensitivity and specificity in differentiating h*MYH9*-RD, t*MYH9*-RD, and bBSS from the other forms of ITs and ITP. Moreover, combining these two cutoff levels increased sensitivity to 98% and specificity to 99%.

Table 4 provides results concerning differentiation of WAS/XLT, CAMT, *CYCS*-RT, and thrombocytopenia with absent radii (TAR) from all other ITs and ITP. An MPD below 2.62 μm, a PDLCR below 9.62%, and a PDSCR above 2.11% had good discriminating capacity in terms of sensitivity and specificity. Combining MPD and PDLCR, sensitivity rose to 96% and specificity rose to 93%.

Discussion

Centralized evaluation of peripheral blood films in a large number of patients with different ITs made a direct comparison of platelet diameters in all disorders identified so far possible for the first time.

Analysis of MPDs confirmed that most ITs have large platelets, although the magnitude of the difference with respect to healthy participants was moderate in most cases, and only patients with h*MYH9*-RD had an MPD more than twice that of the controls. MPD was largely above the upper limit of normal range (as defined by the 97.5th percentiles of platelet diameters in healthy participants: 3.9 μm) only in *MYH9*-RD (in patients with mutations in both the head and the tail of the molecule) and bBSS. Of note, h*MYH9*-RD, t*MYH9*-RD, and bBSS had the highest percentage of large platelets (platelet diameters above the upper limit of normal range), with PDLCRs ranging from 54% to 75%. For classification purposes, we therefore consider it appropriate to describe these conditions as characterized by very large MPDs and a very high proportion of large platelets. More briefly, we can describe these ITs as characterized by giant platelets.

Concerning the other ITs, in 7 forms MPDs were higher than the upper limit of standard deviation of this parameter in healthy participants (3.2 μm): *TUBB1*-related thrombocytopenia (*TUBB1*-RT), gray platelet syndrome (GPS), *FLNA*-related thrombocytopenia (*FLNA*-RT), *GFI1b*-related thrombocytopenia (*GFIb*-RT), mBSS, *ITGA2B/B3*-related thrombocytopenia (*ITGA2B/B3*-RT), and *ACTN1*-related thrombocytopenia (*ACTN1*-RT). In all these conditions, PDLCRs were higher than 20%. Thus, we propose to define these ITs as characterized by large MPDs and a high proportion of large platelets. Otherwise, we can define them as characterized by large platelets.

In FPD-AML, thrombocytopenia Paris-Trousseau (TCPT), XLT with thalassemia (XLTT), *ANKRD26*-RT, congenital thrombocytopenia with radioulnar synostosis (CTRUS), and von Willebrand disease platelet type (VWDP), MPD was higher than in healthy participants but did not differ by more than 25% from the average values of controls. PDLCRs were higher or similar to those of controls. Taking into account the high variability of values within each category of patients, we suggest that these disorders can be classified as characterized by normal or slightly increased platelet size, with normal or increased proportion of large platelets. In brief, these ITs have normal or slightly increased platelet size.

TAR, CAMT, *CYCS*-RT, and WAS/XLT had MPDs below that of controls, and the percentage of PDSCRs was higher than in healthy participants. However, the ranges of values were largely overlapping with those of controls. On the basis of these findings, we believe that these conditions may be described as having normal or slightly reduced platelet size with a normal or slightly increased percentage

Table 3. Platelet diameters for distinguishing IT with giant platelets

	Cutoff	AUC	Sensitivity %	95% CI	Specificity %	95% CI
MPD μm	>3.74	0.9154	86	79 to 91	87	82 to 90
PDDW μm	>4.27	0.8812	80	72 to 86	83	78 to 88
PDLCR %	>39.80	0.9208	85	78 to 91	87	83 to 90
MPD μm and PDLCR %	>3.74 and >39.8	0.9991	98	93 to 99	99	97 to 100

Area under the curve (AUC), sensitivity and specificity of best cutoff levels for MPD, PDDW, and PDLCR identified by receiver operating characteristic analysis in discriminating h*MYH9*-RD, t*MYH9*-RD, and bBSS from all other examined forms of thrombocytopenia.

Table 4. Cutoff values of platelet diameters for distinguishing IT with normal or slightly decreased platelet size

	Cutoff	AUC	Sensitivity %	95% CI	Specificity %	95% CI
MPD μm	<2.62	0.9217	83	58 to 96	90	87 to 93
PDDW μm	<2.85	0.8333	78	52 to 93	83	79 to 86
PDLCR %	<9.62	0.9202	94	71 to 100	80	76 to 84
PDSCR %	>2.11	0.8763	83	58 to 96	86	82 to 89
MPD μm and PDLCR %	<2.62 and <7.21	0.9852	96	87 to 99	93	90 to 95

AUC, sensitivity and specificity of best cutoff levels for MPD, PDDW, PDLCR, and PDSCR identified by receiver operating characteristic analysis in discriminating WAS/XLT, *CYCS*-RT, CAMT, and TAR from all other forms of thrombocytopenia.

of small platelets. For classification purposes, TAR, CAMT, *CYCS*-RT, and WAS/XLT may be defined as having normal or slightly decreased platelet size.

Table 5 reports the new classification that emerged from the precise measurement of platelet diameters and the percentage of platelets larger or smaller than specific threshold values. We emphasize that it identifies distinct categories of diseases, whereas in reality, the size of the platelets in ITs varies in a continuous manner from values much higher to values slightly lower than those of controls. Moreover, platelet size varies in patients with the same disorder. Thus, this classification, as with many other disease classifications, is rather artificial and is intended to be used as a scholastic tool. We also note that, for some disorders, we were able to examine only a few patients, or even only one. Thus, a definitive classification of these very rare forms requires the evaluation of additional patients.

Our study aimed to better define platelet phenotypes in ITs and also to evaluate whether platelet diameters may be used as a diagnostic tool for differential diagnosis of ITs. This matter has been addressed by two studies that measured MPDs in 35 and 46 patients with inherited macrothrombocytopenias and evaluated the ability of platelet diameters to discriminate between these conditions and ITP. The first study found that an MPD larger than 3.3 μm differentiated *MYH9*-RT, mBSS, and bBSS from ITP with 89% sensitivity and 88% specificity.[7] The second study, evaluating a different patient population, found that the same cutoff value had 67% specificity and 75% sensitivity in differentiating these conditions from ITP.[5]

This study confirmed that MPD has good diagnostic accuracy in distinguishing ITs with giant platelets (h*MYH9*-RD, t*MYH9*-RD, and bBSS) not only from ITP but also from all other ITs. Indeed, an MPD larger than 3.74 μm had 86% sensitivity and 87% specificity in this respect. Of note mBSS, in most cases deriving from a Bolzano mutation, was not included within the group of disorders distinguishable from ITP by this parameter because MPD of affected patients was lower in this large case series than in previous smaller studies.[5,7] The results were quite similar to MPD measured in ITP. A new finding of our study was the demonstration that MPD was able to distinguish ITs with normal or slightly decreased platelet size from ITP and the other forms of ITs. In fact, an MPD smaller than 2.62 μm had 83% sensitivity and 90% specificity in this regard.

Table 5. Classification of ITs according to MPDs and the percentage of large platelets

ITs	MPD (μm)	Large platelets (%)	
With giant platelets	>4	PDLCR >50%	h*MYH9*-RD
			bBSS
			t*MYH9*-RD
With large platelets	>3.2	PDLCR >20%	*TUBB1*-RT
			GPS
			FLNA-RT
			GFI1b-RT
			mBSS
			ITGA2B/B3-RT
			ACTN1-RT
With normal or slightly increased platelet size	>2.6	And/or PDLCR >5%	FDP-AML
			TCPT
			XLTT
			ANKRD26-RT
			CTRUS
			VWDP
With normal or slightly decreased platelet size	<2.6	And/or SDCR >5%	TAR
			CAMT
			CYCS-RT
			XLT/WAS

Another new finding was that the percentage of large platelets had good diagnostic accuracy in differentiating ITs with giant platelets from all other investigated forms of thrombocytopenia. In particular, a percentage of PDLCRs higher than 39.8% had 85% sensitivity and 87% specificity in this respect. Moreover, combining an MPD larger than 3.7 μm and a PDLCR higher than 39.8% increased sensitivity and specificity to near 100%.

We also showed that both PDSCR and PDLCR can be used to recognize ITs with normal or slightly decreased platelet size. A PDSCR above 2.11% had 83% sensitivity and 86% specificity in differentiating these forms from ITP and all other ITs, whereas a PDLCR below 9.62% had 94% sensitivity and 80% specificity. The joint use of MPD and PDLCR increased sensitivity and specificity to 96% and 93%, respectively.

Thus, in our series of 376 patients with ITs, evaluation of blood films would have been a valuable diagnostic tool for recognizing the 156 patients with giant platelets or normal to slightly decreased platelet size.

An obvious objection to the proposal of using platelet diameters for diagnostic purposes is that measuring this parameter by microscope evaluation of blood films is time consuming and, as a consequence, difficult to apply in clinical practice. The availability of cell counters that reliably measure platelet size and the percentage of platelets larger or smaller than specific cutoff values would probably solve this problem. As already discussed, these instruments are not yet available, and we have to wait for the next generation of instruments to verify whether they are as efficient as microscope evaluation of blood films in differential diagnosis of ITs. In the meantime, we have to continue using the microscope for assessing platelet dimensions. This task is made easier by the fortunate coincidence that 3.9 μm, the cutoff value for large platelets, is about half the diameter of normal erythrocytes on blood films. Of note, results of empirical evaluation of PDLCR by visually comparing the diameters of platelets with those of red cells showed a very strong correlation with the values obtained by software-assisted image analysis. Comparing the size of platelets with those of erythrocytes may therefore be a simple and quick method for getting a first impression of PDLCR and to decide whether a more accurate evaluation of platelet diameter might be worthwhile. Indeed, a PDLCR higher than 40% or smaller than 10% supports a diagnosis of an IT with giant platelets and an IT with

normal or slightly decreased platelet size, respectively, whereas PDLCRs within these two limits are compatible with ITP as well as with ITs with large platelets and with normal or slightly increased platelet size.

One flaw in our study is that we studied only one or a very few patients with some forms of ITs. Because of the high variability of platelet diameters observed in each IT, it may be that the values we reported here are not fully representative of these poorly investigated disorders. Thus, it might happen that the proposed classification of ITs according to platelet diameters is amended in the future by studying additional patients. Statistical analyses also suffered from the dearth of some forms of IT, and the study of additional patients is therefore required to better define the size of platelets in rare disorders. Finally, we cannot exclude that differences in the preparation of blood films in different centers affected the evaluation of platelet diameters.

In conclusion, the precise measurement of platelet diameters in the largest series of patients with ITs ever collected and including all known disorders allowed us to propose a new classification of these disorders based on platelet size. Moreover, it allowed us to identify MPD, as well as the percentage of large and small platelets, as useful parameters for differential diagnosis of ITs.

Acknowledgments

This work was supported by grant no. GGP10089 from Telethon Foundation Italy.

Authorship

Contribution: P.N., A.P., A.S., M.S., G.L., G.R., L.D.N., P.G., P.G.H., N.P.-M., S.K., M.C., J.B., E.D.C., U.R., and F.F. investigated patients and provided study materials; E.C., F.M., V.B., C.C., and S.B. analyzed blood films; E.C. assembled data; G.B. analyzed data; P.N., G.B., A.P., and C.L.B. wrote the manuscript; and all authors had access to primary clinical data and revised and gave final approval to the manuscript.

Conflict-of-interest disclosure: The authors declare no competing financial interests.

Correspondence: Carlo L. Balduini, Fondazione Istituto Di Ricovero e Cura a Carattere Scientifico Policlinico San Matteo, Viale Golgi 19, Pavia, Italy; e-mail: c.balduini@smatteo.pv.it.

References

1. Balduini CL, Savoia A, Seri M. Inherited thrombocytopenias frequently diagnosed in adults. *J Thromb Haemost.* 2013;11(6):1006-1019.
2. Balduini CL, Savoia A. Genetics of familial forms of thrombocytopenia. *Hum Genet.* 2012;131(12):1821-1832.
3. Pecci A, Gresele P, Klersy C, et al. Eltrombopag for the treatment of the inherited thrombocytopenia deriving from MYH9 mutations. *Blood.* 2010;116(26):5832-5837.
4. Pecci A, Barozzi S, d'Amico S, Balduini CL. Short-term eltrombopag for surgical preparation of a patient with inherited thrombocytopenia deriving from MYH9 mutation. *Thromb Haemost.* 2012;107(6):1188-1189.
5. Noris P, Klersy C, Gresele P, et al; Italian Gruppo di Studio delle Piastrine. Platelet size for distinguishing between inherited thrombocytopenias and immune thrombocytopenia: a multicentric, real life study. *Br J Haematol.* 2013;162(1):112-119.
6. Latger-Cannard V, Hoarau M, Salignac S, Baumgart D, Nurden P, Lecompte T. Mean platelet volume: comparison of three analysers towards standardization of platelet morphological phenotype. *Int J Lab Hematol.* 2012;34(3):300-310.
7. Noris P, Klersy C, Zecca M, et al. Platelet size distinguishes between inherited macrothrombocytopenias and immune thrombocytopenia. *J Thromb Haemost.* 2009;7(12):2131-2136.
8. Pecci A, Panza E, Pujol-Moix N, et al. Position of nonmuscle myosin heavy chain IIA (NMMHC-IIA) mutations predicts the natural history of MYH9-related disease. *Hum Mutat.* 2008;29(3):409-417.
9. Pecci A, Klersy C, Gresele P, et al. MYH9-related disease: a novel prognostic model to predict the clinical evolution of the disease based on genotype-phenotype correlations. *Hum Mutat.* 2014;35(2):236-247.
10. Noris P, Perrotta S, Bottega R, et al. Clinical and laboratory features of 103 patients from 42 Italian families with inherited thrombocytopenia derived from the monoallelic Ala156Val mutation of GPIbα (Bolzano mutation). *Haematologica.* 2012;97(1):82-88.
11. George JN, Woolf SH, Raskob GE, et al. Idiopathic thrombocytopenic purpura: a practice guideline developed by explicit methods for the American Society of Hematology. *Blood.* 1996;88(1):3-40.
12. British Committee for Standards in Haematology General Haematology Task Force. Guidelines for the investigation and management of idiopathic thrombocytopenic purpura in adults, children and in pregnancy. *Br J Haematol.* 2003;120(4):574-596.
13. Massaad MJ, Ramesh N, Geha RS. Wiskott-Aldrich syndrome: a comprehensive review. *Ann N Y Acad Sci.* 2013;1285:26-43.
14. Biino G, Gasparini P, D'Adamo P, et al. Influence of age, sex and ethnicity on platelet count in five Italian geographic isolates: mild thrombocytopenia may be physiological. *Br J Haematol.* 2012;157(3):384-387.